UNIVERSIDADE FEDERAL DE OURO PRETO

ESCOLA DE MINAS

DEPARTAMENTO DE GEOLOGIA

TRABALHO DE CONCLUSÃO DE CURSO

INFLUENCE OF CARTOGRAPHIC REPRESENTATION OF LANDSLIDES' FEATURES ON SUSCEPTIBILITY MODELS: ANALYSIS OF SHALLOW AND DEEP TRANSLATIONAL SLIDES IN THE REGION OF OURO PRETO/MG, BRAZIL

Jefferson Alves Araujo Junior

MONOGRAFIA nº 389

Ouro Preto, Fevereiro de 2021

INFLUENCE OF CARTOGRAPHIC REPRESENTATION OF LANDSLIDES' FEATURES ON SUSCEPTIBILITY MODELS: ANALYSIS OF SHALLOW AND DEEP TRANSLATIONAL SLIDES IN THE REGION OF OURO PRETO/MG, BRAZIL

FUNDAÇÃO UNIVERSIDADE FEDERAL DE OURO PRETO

Reitora

Prof.ª Dr.ª Cláudia Aparecida Marliére de Lima

Vice-Reitor

Prof. Dr. Hermínio Arias Nalini Júnior

Pró-Reitora de Graduação

Prof.ª Dr.ª Tânia Rossi Garbin

ESCOLA DE MINAS

Diretor

Prof. Dr. Issamu Endo

Vice-Diretor

Prof. Dr. Hernani Mota de Lima

DEPARTAMENTO DE GEOLOGIA

Chefe

Prof. M.Sc. Edison Tazava

MONOGRAFIA

Nº 389

INFLUENCE OF CARTOGRAPHIC REPRESENTATION OF LANDSLIDES' FEATURES ON SUSCEPTIBILITY MODELS: ANALYSIS OF SHALLOW AND DEEP TRANSLATIONAL SLIDES IN THE REGION OF OURO PRETO/MG, BRAZIL

Jefferson Alves Araujo Junior

Orientador

Prof. Dr. Cesar Falcão Barella

Co-Orientador

M.Sc. Cahio Guimarães Seabra Eiras

Monografia do Trabalho de Conclusão de curso apresentado ao Departamento de Geologia da Escola de Minas da Universidade Federal de Ouro Preto como requisito parcial para avaliação da disciplina Trabalho de Conclusão de Curso – TCC 402, ano 2020/1.

OURO PRETO

2021

Universidade Federal de Ouro Preto – http://www.ufop.br
Escola de Minas - http://www.em.ufop.br
Departamento de Geologia - http://www.degeo.ufop.br/
Campus Morro do Cruzeiro s/n - Bauxita
35.400-000 Ouro Preto, Minas Gerais
Tel. (31) 3559-1600, Fax: (31) 3559-1606

Revisão geral: Jefferson Alves Araujo Junior

Catalogação elaborada pela Biblioteca Prof. Luciano Jacques de Moraes do
Sistema de Bibliotecas e Informação - SISBIN - Universidade Federal de Ouro Preto

SISBIN - SISTEMA DE BIBLIOTECAS E INFORMAÇÃO

A663i Araujo Junior, Jefferson Alves.
Influence of cartographic representation of landslides' features on susceptibility models [manuscrito]: analysis of shallow and deep translational slides in the region of Ouro Preto/MG, Brazil. / Jefferson Alves Araujo Junior. - 2021.
48 f.: il.: color., gráf., tab., mapa.

Orientador: Prof. Dr. Cesar Falcão Barella.
Coorientador: Me. Cahio Guimarães Seabra Eiras.
Monografia (Bacharelado). Universidade Federal de Ouro Preto. Escola de Minas. Graduação em Engenharia Geológica .

1. Geotecnia. 2. Deslizamentos (Geologia). 3. Mapeamento de susceptibilidade. 4. Métodos estatísticos. I. Barella, Cesar Falcão. II. Eiras, Cahio Guimarães Seabra. III. Universidade Federal de Ouro Preto. IV. Título.

CDU 624.131.537

Bibliotecário(a) Responsável: Sione Galvão Rodrigues - CRB6 / 2526
Catalogação: ficha@sisbin.ufop.br

Ficha de Aprovação

TRABALHO DE CONCLUSÃO DE CURSO

TÍTULO: Influence of cartographic representation of landslides' features on susceptibility models: Analysis of shallow and deep translational slides in the region of Ouro Preto/MG, Brazil

AUTOR: JEFFERSON ALVES ARAUJO JUNIOR

ORIENTADOR: Cesar Falcão Barella

COORIENTADOR: Cahio Guimarães Seabra Eiras

Aprovada em: 19 de fevereiro de 2021

BANCA EXAMINADORA:

Prof. Dr. Cesar Falcão Barella	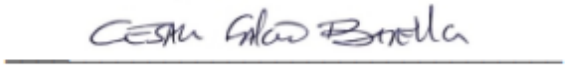	DEAMB/UFOP
Prof. Dr. Frederico Garcia Sobreira	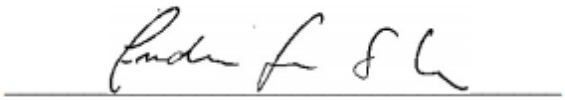	DEAMB/UFOP
Prof. M.Sc. Mateus Oliveira Xavier	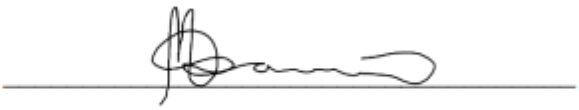	DEARQ/UFOP

Ouro Preto, 19/02/2021

Agradecimentos

Agradeço ao meus pais, Maiza e Jefferson, pelo apoio incondicional.

Aos meus orientadores Cesar e Cahio pelos ensinamentos e oportunidades.

À AngloGold Ashanti unidades Serra Grande e Córrego do Sítio pelo crescimento profissional.

À Montanuniversität Leoben pela experiência única e ensino excepcional.

À Geoconsultoria Jr. Pelo aprendizado e trabalho em equipe.

Ao Serviço Geológico do Brasil (CPRM) e CNPq pelo apoio institucional.

À Universidade Federal de Ouro Preto, à Escola de Minas e Departamento de Geologia pelo ensino público de qualidade.

À grandiosa República Boite Casablanca por ser uma verdadeira escola de vida.

SUMMARY

ILUSTRATION INDEX

TABLE LIST

Abstract

The influence of cartographic representation of small and large-sized landslides, through points and polygons, was evaluated in statistical models of susceptibility, in the central region of the municipality of Ouro Preto, Brazil. 18 models were produced using an inventory with 57 features mapped with an Unmanned Aerial Vehicle. The area and volume of these features were determined, which allowed the establishment of a statistical correlation between both parameters, with a coefficient of determination (R^2) of 0.9687. Three divisions of the dependent variables, between the training and test subgroups, were adopted based on the slide's volume. In each of these divisions, the following cartographic representations were adopted: polygon, point in the centre of mass, and random point inside the slide's features. The conditioning factors used in the modelling were: lithological units, slope angle, geomorphological units, slope aspect, and land use. The informative value method was used in the construction of the models, which were validated through the success and prediction curves. The results demonstrated that landslides of small and large sizes are differently influenced by the conditioning factors, and the cartographic representation changes the influence of the factors for the same sliding feature. A polygonal cartographic representation and a balanced partition of the dependent variables (large and deep landslides in both training and test subgroups) were demonstrated to produce the best results. The worst result was obtained using a point and random cartographic representation and a partition of dependent variables with a predominance of large and deep landslides in the training subgroup. Thus, the adoption of different cartographic representations to map the features of landslides in regions that register movements of different magnitudes may interfere in the quality of the susceptibility models and in the spatial arrangement of the susceptibility classes, producing distinctly different maps for the same locality.

Key words: Landslide, Susceptibility mapping, Bivariate statistics, Landslide inventory, Landslide volume.

Resumo

A influência da representação cartográfica de deslizamentos de pequeno e grande porte, por meio de pontos e polígonos, foi avaliada em modelos estatísticos de suscetibilidade, na região central do município de Ouro Preto, Brasil. 18 modelos foram produzidos a partir de um inventário com 57 feições de cicatrizes mapeadas com um Veículo Aéreo Não Tripulado. Foram determinados a área e o volume dessas feições, o que permitiu estabelecer uma correlação estatística entre os dois parâmetros com um coeficiente de determinação (R^2) de 0,9687. Três divisões das variáveis dependentes, entre os subgrupos de treino e teste, foram adotadas com base no volume dos escorregamentos. Em cada uma dessas divisões, as seguintes representações cartográficas foram adotadas: polígono, ponto no centro de massa e ponto aleatório dentro das feições dos escorregamentos. Os fatores condicionantes utilizados na criação dos modelos foram: unidades litológicas, declividade, unidades geomorfológicas, aspecto e uso e ocupação. O método do valor informativo foi utilizado na construção dos modelos, que foram validados através das curvas de sucesso e de predição. Os resultados encontrados evidenciaram que escorregamentos de pequeno e grande porte são diferentemente influenciados pelos fatores condicionantes, além da representação cartográfica alterar a influência dos fatores para uma mesma feição de escorregamento. O melhor resultado encontrado utilizou uma representação cartográfica poligonal e uma partição equilibrada das variáveis dependentes (grandes e profundos escorregamentos em ambos os subgrupos de treino e de teste). O pior resultado encontrado utilizou uma representação cartográfica pontual e aleatória e uma partição das variáveis dependentes com predominância de grandes e profundos escorregamentos no subgrupo de treino. Dessa forma, pode-se concluir que a adoção de diferentes representações cartográficas para mapear as feições de escorregamentos em regiões que registram movimentos de diferentes magnitudes pode interferir na qualidade dos modelos de susceptibilidade elaborados e no arranjo espacial das classes de susceptibilidade, produzindo mapas distintos para uma mesma localidade.

Palavras-Chave: Escorregamento, Mapeamento de susceptibilidade, Métodos estatísticos bivariados, Inventário de escorregamentos, Volume de escorregamentos.

CHAPTER 1

INTRODUCTION

1.1 PRESENTATION

Landslide susceptibility mapping assesses the natural predisposition of a terrain to landslide development and assists in landscape planning and management through the identification of areas more prone to landslides (Huang & Zhao 2018; Kadavi *et al.* 2018; Pham & Prakash 2019; Nohani *et al.* 2019; Pham *et al.* 2020). These maps have been produced since the 1970s and landslide inventories are used in more than 80% of susceptibility studies (Reichenbach *et al.* 2018). The predictive capacity of susceptibility models based on statistical methods is dependent on the bases used for their generation, and landslide inventories are of fundamental importance for the creation of predictive models (Aditian *et al.* 2018; Huang & Zhao 2018; Pourghasemi *et al.* 2018; Kadavi *et al.* 2018; Nohani *et al.* 2019; Pham *et al.* 2020).

The cartographic representation of features left in the landscape by old landslides usually occurs by the adoption of a vector symbology, in the form of points, lines or polygons. Its choice is arbitrary (Oliveira 2010) and will depend, principally, on the mapping scale, the objective of the inventory map, the availability of data, and the personal choice of the operator. The representation of landslides by lines presents an illustrative character and can be used to corroborate qualitatively the zones of highest susceptibility. Therefore, it has little practical use in the construction of statistically based predictive models.

When the objective of the inventory is a susceptibility map, it is preferable to use points, or polygons. However, the influence of these graphical aspects on susceptibility statistics, is less debated than studies comparing different statistical modelling approaches. According to Oliveira *et al.* (2009), predictive models are more sensitive to the transformation of the input-dependent variable, that is, the inventoried features, than variation in statistical methods.

When choosing to use polygons, it is possible to map only the rupture zone, excluding the accumulation zone from the analysis, or the entire moved unit, formed by the depletion and accumulation zone. In the first case, which is most common in the literature, the susceptibility models generated do not guarantee the modelling of the accumulation zones, which are essential in more detailed studies, since the propagation of unstable material can cause damage and harm (Garcia 2012).

The second case may incur severe biases in the development of the statistical model, especially if a large part of the registered movement is present across a large distance, which is due to the inclusion in the model of dispensable parameters for the development of the phenomena being

investigated (Thiery *et al.* 2007). This becomes clear when a landslide moves under the influence of a specific lithological unit, located near the depletion zone, but due to the distance of impact being large, another lithological unit, which is not linked to the development of the movement, is incorporated in the analysis. Thus, although this procedure can allow the incorporation of the zones of impact in the analysis, it can also culminate in decreased statistical robustness of the model and, consequently, in the enlargement of the zone of high susceptibility. This fact is related to the lack of dependence between the factors of predisposition considered and the listed features (Barella 2016).

The representation of listed features through points is usually easier and faster than polygons. This cartographic process is present in several mapping works (Aditian *et al.* 2018; Kadavi *et al.* 2018; Nohani *et al.* 2019; Pham *et al.* 2020). Generally, this arises because of the rapid attendance at landslides of the municipal civil defence, who allocate approximate coordinates in sheets and analogical spreadsheets, mainly in underdeveloped countries. When this cartographic representation is an option, and since the operator has at his disposal polygonal features, the points are commonly located in the centroids of the unstable regions due to the operational ease of doing this in geographic information systems (Zhu *et al.* 2018, Chen & Li 2020; Pham *et al.* 2020).

Point-based and polygonal features both have advantages and disadvantages within a statistical approach of susceptibility analysis, and it is up to the operator to decide the feature capable of representing the landslide most accurately. The point approach promotes an analogous treatment between large and small sliding features, avoids the uncertainties related to the spatial delimitation of old features and/or features covered by dense vegetation, reduces the spatial correlation of dependent variables, and produces robust statistical models of susceptibility (Carrara 1993; Atkinson *et al.* 1998; Van Deneeckhaut *et al.* 2006; Thiery *et al.* 2007; Zêzere *et al.* 2009; Petschko *et al.* 2013; Heckmann *et al.* 2014; Petschko *et al.* 2014; Goetz *et al.* 2015).

The polygonal approach represents the real way landslides occur in the landscape, produces more spatially concordant models when more than one statistical technique is used, does not ignore the effect of the magnitude of landslides in heterogeneous environments, and tends to produce more robust predictive results when the inventory presents broad and deep features (Guri *et al.* 2015; Oliveira *et al.* 2015; Zêzere *et al.* 2017; Barella *et al.* 2019).

1.2 STUDY AREA

The study area is 46.77 km², located in the south eastern portion of Brazil, in the state of Minas Gerais, the central region of the municipality of Ouro Preto; the area's elevation is between 898.25 m and 1591.35 m; throughout the area, 57 landslide features were cataloged (Figure 1.1). In

Ouro Preto, the anthropic activity that has most modified the landscape and relief was mining, which occurred in the 18th century and severely affected the stability of many slopes (Sobreira & Fonseca 2001; Sobreira 2014; Paula & Castro 2015; Xavier 2018).

The relief of the region is intensely marked by structural control, where the presence of extensive erosive escarpments, ridges with ravine slopes and embedded valleys, as well as hilltops with flat bottom valleys occur (Fontes 1999). Approximately 53% of the relief is from hills with an altitude varying between 1591.35 and 898.25 meters. The highest mountains have an elevation of 693.1 meters in relation to the lowest part of the study area. The predominant slope is approximately 20° but exceeding 60° in places.

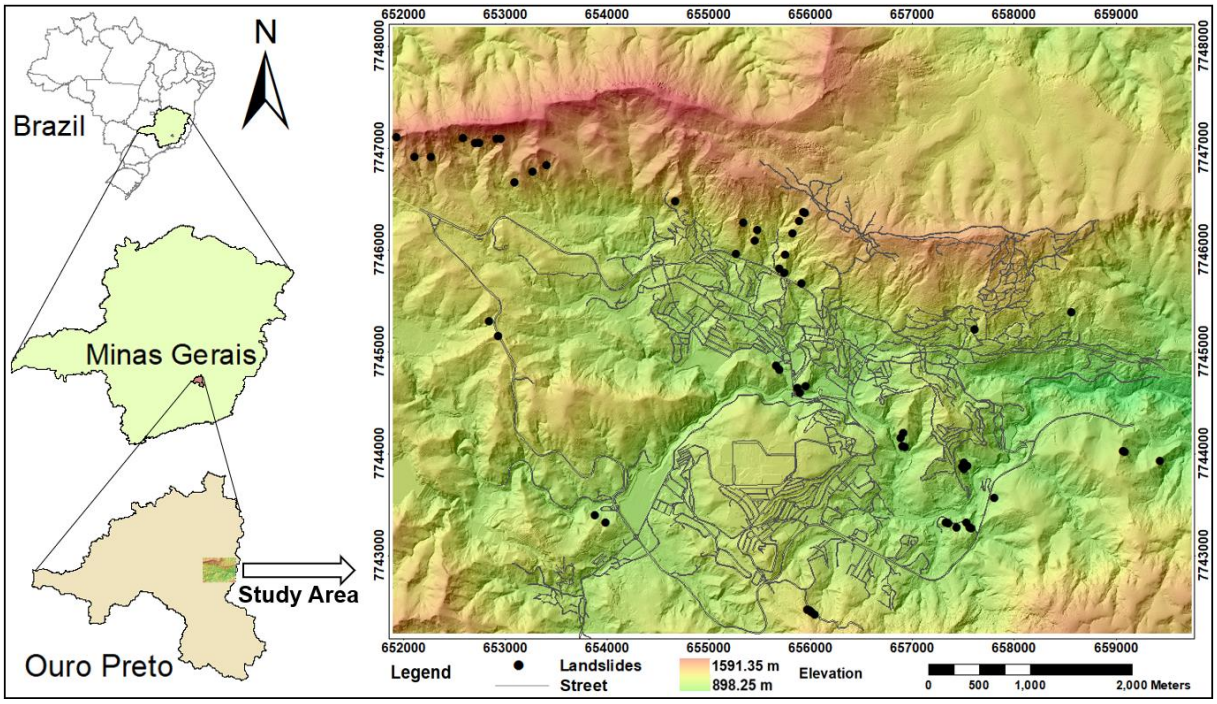

Figure 1.1 - Location of the study area with Digital Elevation Model shaded on relief and the cataloged landslides features.

Located in the southeast of the Iron Quadrangle, the region is composed predominantly of metamorphic rocks (e.g., phyllite, banded iron formation, quartzite, schist). Lithology is one of the main conditioning factors for the occurrence of landslides in the study area. The local rocks exhibit foliation that, when associated with the steep relief and high incidence of rainfall in the region, contributes to the occurrence of landslides. The schists of the Nova Lima group are highly altered, while the phyllites of the Piracicaba group have low resistance to denudational processes, and many constructions, which promote alterations in the relief (e.g., cuts and embankments, concentration of

surface water flows), are constructed over them (Castro 2006). In itabirites on the southern flank of the Ouro Preto mountain range, the most prominent geomorphologic domain in Figure 1, which is aligned predominantly in the E-W direction, thickening of much of the domain and older scars can be observed.

Landslides in the study area are predominantly translational and are associated with structurally controlled failure mechanisms by weakness surfaces (Varnes 1978). These surfaces generally occur in three geostructural contexts (Barella *et al.* 2019): (i) contact between rock and residual soil or colluvium; (ii) structures in saprolitic soils (foliation or schistosity); and (iii) variation of shear strength of different lithological layers.

1.3 OBJECTIVE

The objective of this study was to evaluate the influence of the cartographic representation of landslides on the predictive capacity of statistical susceptibility models in a region marked by the occurrence of translational landslides of small and large magnitude. Specific objectives:

- Assess the influence of the relationship between the magnitude of landslides and the punctual and polygonal cartographic representation on the predictive capacity of susceptibility models.

- Assess the influence of the punctual and polygonal representation of landslides features in the partition of the dependent variables (train and test subgroups).

- Assess the locational effect of the point along landslides of different magnitudes and the effect caused on the predictive capacity of susceptibility models.

CHAPTER 2

GEOLOGICAL CONTEXT

2.1 REGIONAL GEOTECTONIC CONTEXT

The Iron Quadrangle (IQ) is in the southern region of the São Francisco Craton (SFC) and is surrounded by verging orogenetic belts to its interior (Rossi 2014). The IQ is composed of two tectonic environments (Rossi 2014; Almeida 1977): SFC and the Araçuaí Belt. The SFC is tectonically classified as a stable region, where erosive processes predominate without the formation of new mountain ranges. It has not undergone significant tectonic deformations since the Paleoproterozoic and its formation occurred at approximately 2 Ga, at the end of the Trans-Amazonian Cycle (Barbosa & Barbosa 2017). The Araçuaí Belt is one of the regions around the SFC; its fold and thrust belts were originated from epigenetic movements that occurred during the Brasiliano orogeny cycle (Almeida 1977). The study area region is in IQ's southeast; it is composed of neo-Archean greenstone belts that are surrounded by gneiss complexes overlaid by Paleoproterozoic metasedimentary rocks.

2.2 STRATIGRAPHY

The stratigraphic units in the IQ region have ages varying from the Archean to the Proterozoic (Carneiro *et al.* 1995). The oldest layers are composed of crystalline rocks, followed by the deposition of three units: the Archean meta-volcanosedimentary sequence Rio das Velhas Supergroup, the Paleoproterozoic Minas Supergroup, and the Itacolomi Group (Rossi 2014; Alkmim & Marshak 1998; Dorr 1969). On a regional scale, the following larger groups can be defined (Lobato *et al.* 2005): (i) Archean granite-gneissic terrains, (ii) Archean volcanic-sedimentary sequences, (iii) Proterozoic sedimentary and volcanic-sedimentary cover sequences, and (iv) sedimentary recent coverings. Figure 2.1 shows the geological map of the study area, while Table 2.1 is a simplified stratigraphic chart.

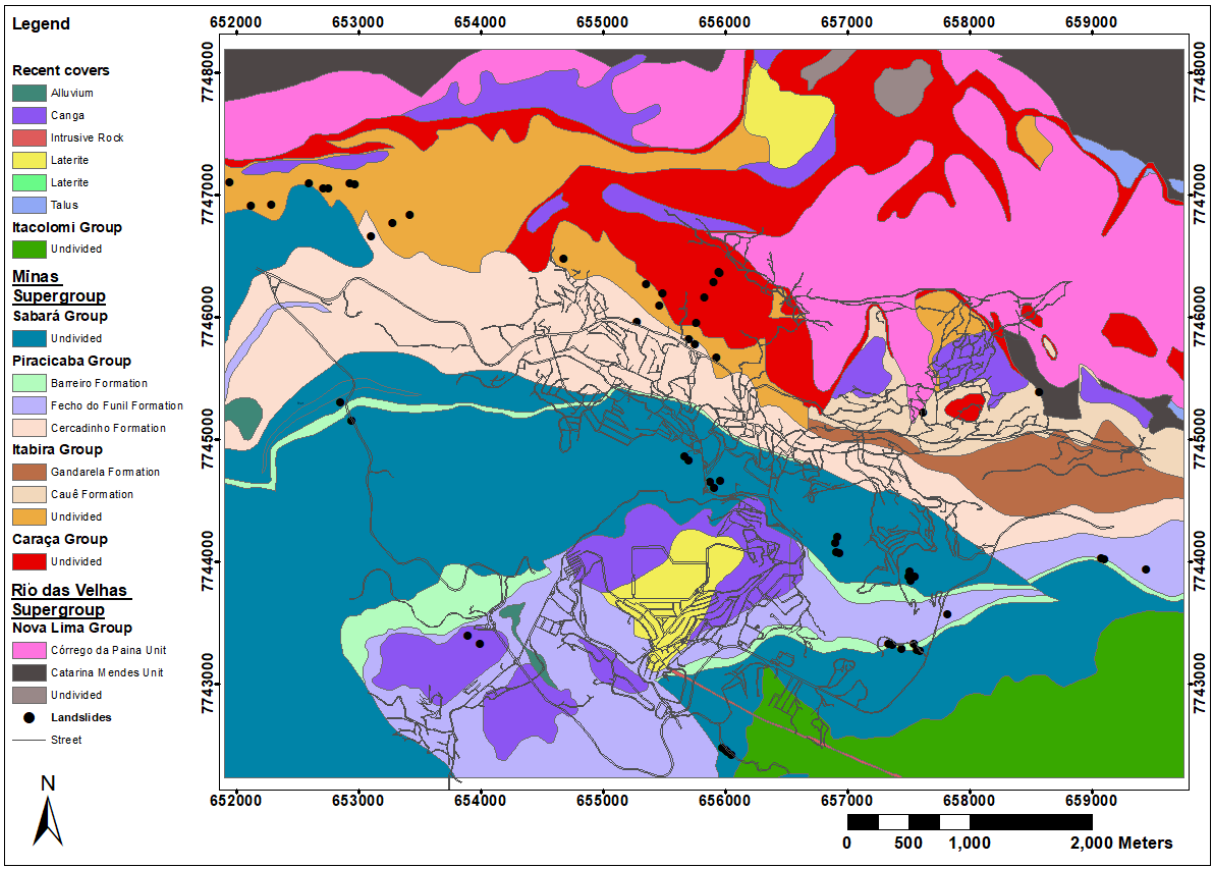

Figure 2.1 - Simplified geological map of the study area.

Table 2.1 - Simplified stratigraphic chart (modified from Alkmim & Marshak 1998).

Supergroup	Group	Formation
	Itacolomi	
Minas	Sabará	
	Piracicaba	Barreiro Taboões Fecho do Funil Cercadinho
	Itabira	Gandarela Cauê
	Caraça	Batatal Moeda
Rio das Velhas	Nova Lima	Córrego da Paina Unit Catarina Mendes Unit
Metamorphic Complexes		

2.2.1 Archean Granite-Gneissic terrains

The IQ's basement is composed of Archean crystalline rocks (Rossi 2014) and it is divided into complexes: Bonfim (Machado & Carneiro 1992), Belo Horizonte (Machado & Noce 1993), Caeté, Santa Bárbara and Bação (Machado *et al.* 1992). The basement is polyphasic deformed and the metamorphism was medium to superior amphibolite facies conditions, followed by greenschist facies conditions (Rossi 2014). The unit is mainly composed of orthogneisses, granites, granodiorites, amphibolites, and intrusions of mafic and ultramafic rocks (Herz 1970; Carneiro 1992). The basement rocks are isotropic or foliated, and it occasionally has secondary structures (Rossi 2014). In the study area, there are no outcrops of this unit.

2.2.2 Rio das Velhas Supergroup

The Rio das Velhas Supergroup is composed of meta-volcanosedimentary sequences that characterize the Archean greenstone-belt (Machado *et al.* 1989, 1992; Dorr 1969). This supergroup occurs across the east-southeast border of the SFC. It is tectonically disposed above the granite-gneissic Archean unit (Almeida 2004) and its rocks are mainly shales generated from hydrothermal alterations and metamorphism of mafic and ultramafic rocks or sediments (Hasui *et al.* 2012; Zucchetti *et al.* 2000).

2.2.3 Nova Lima Group

The Nova Lima Group is mainly composed of shales with wide lithological variability and different stratification patterns (Fontes 2011). The group comprises metasedimentary rocks of carbonate and siliciclastic composition as well as banded iron formations (BIFs) of the Algoma type (Rossi 2014). The group's lithologies are mainly in the north of the study area. The shales of the Nova Lima Group exhibit high degrees of weathering and patterns of anisotropy. Due to these and other characteristics, these rocks are sensitive to the occurrence of landslides (Xavier 2018; Fontes 2011). The Córrego da Paina and Catarina Mendes units are outcrops in the study area.

2.2.4 Minas Supergroup

The Minas Supergroup is a Paleoproterozoic meta-sedimentary sequence; it and Rio das Velhas Supergroup contact has an angular unconformity (Rossi 2014; Dorr 1969). Its rocks are mainly composed of clastic and chemical sediments from the erosion of the granite-gneiss complex and the Rio das Velhas Supergroup (Hasui *et al.* 2012). Trans-Amazonian and Brasiliano orogeny cycles are

responsible for generating mountain ranges and metamorphosing the Minas Soupergroup's sedimentary rocks (Alderete 2020; Hurley *et al.* 1967). Its stratigraphic organization is constituted by shales, quartzites, dolomites, and BIFs, being divided into five large units (Rossi 2014; Dorr 1969; Almeida 2004): clastic sediments from the Tamanduá Group, clastic sediments from the Caraça Group, chemical sediments from the Itabira Group, clastic and chemical sediments from the Piracicaba Group, and flysh sediments from the Sabará Group.

2.2.5 Caraça Group

The Caraça Group is composed of the Moeda and Batatal formations. The Moeda Formation is composed predominantly of metaconglomerates, phyllites, and quartzites with varying sericite content (Rossi 2014; Dorr 1969). The Batatal formation is mainly composed of phyllites and BIFs (Maxwell 1958; Dorr 1969). The rocks of these units are in the hills of the study area's north. Quartzites tend to break in form of plates due to their well-defined schistosity (i.e., translational landslide, topple, or rockfall). Furthermore, the phyllites are relevant in the geological-geotechnical context of the area because its low resistance to weathering and low permeability (Sobreira & Araújo 1992).

2.2.6 Itabira Group

The Itabira Group is composed of the Cauê and Gandarela formations (Dorr 1969). The Cauê Formation is composed of BIFs, as well as phyllite and marl lenses (Machado et al 1996; Dorr 1969). The Gandarela Formation is gradually superimposed on the Cauê Formation (Dorr 1969) and it is composed mainly of dolomitic marbles, BIFs, and phyllites (Hasui *et al.* 2012). The Cauê Formation appears geomorphologically as convex profile slopes on the Ouro Preto´s hill, these slopes tend to be covered by a limonitic cover (as a result of in situ weathering); furthermore, they are highly vulnerable to water erosion (Fontes 2011). In theory, the BIFs of this unit is not overly sensitive to the occurrence of mass wasting, however, due to weathering and contact with other less permeable units, they become very susceptible to events (Ferreira 2018; Xavier 2018). The Gandarela Formation generally occurs in the bottom of valleys, tending to form steep walls on the study area's east.

2.2.7 Piracicaba Group

The Piracicaba Group is a clastic sequence, divided from the bottom to the top in the Cercadinho, Fecho do Funil, Taboões, and Barreiro formations (Rossi 2014; Dorr *et al.* 1957). The Cercadinho Formation's lithologies are silver phyllite, dolomitic phyllite, ferruginous phyllite,

quartzite, ferruginous quartzite, and dolomite (Rossi 2014; Dorr 1969). The alternation between quartzite and phyllite packages is a characteristic of this unit (Aderete 2020; Fontes 2011). The areas in which the quartzites of this unit predominate are very weathered and in escarpment relief, while those that predominate phyllites tend to more depressed reliefs. The ferruginous quartzite and silver phyllite of this unit have a low resistance to denudation processes (Xavier 2018; Sobreira & Araújo 1992). The Feixo do Funil Formation is composed of dolomitic phyllites, phyllites, and dolomite lenses (Alderete 2020; Rossi 2014; Simmons 1968). The Taboões and Barreiro Formations are predominantly composed of quartzites and graphite phyllites respectively (Alderete 2020; Rossi 2014; Pomerene 1958a; Pomerene 1958b). The quartzites of the Barreiro Formation are discontinuous, weathered and of low resistance; thus, this is a formation sensitive to wasting processes (Xavier 2018; Sobreira & Araújo 1992).

2.2.8 Sabará Group

The Sabará Group has a thickness of 3.5 km, being the thickest sequence of the Minas Supergroup (Alderete 2020; Reis *et al.* 2002). It consists of shales, phyllites, metarenites, metavolcanoclastics, metaconglomerates, and metadiamictites (Rossi 2014). It is the sequence with the greatest spatial distribution throughout the study area. The existence of embankments without signs of instability, with vertical cutting slopes of more than 10 meters in height, indicates low susceptibility of the rocks of this group to mass wasting processes (Fontes 2011). However, if the dip direction of the foliation is in the same direction of these cutting slopes it will make the embankments of this and other units overly sensitive to mass wasting processes (Ferreira 2018; Fernandes & Amaral 1996).

2.2.9 Itacolomi Group

The Itacolomi Group is the unit that constitutes the top of the region's stratigraphic sequence (Dorr 1969). The main rocks in this unit are quartzites, metaconglomerates, and phyllites (Alkimim & Martins-Neto 2012). The Itacolomi Group contact with the Sabará, Barreiro, and Fecho do Funil units has an angular unconformity (Rossi 2014). The rocks of this group occur in the southern region of the study area, in the form of large outcrops. A dike across the rocks of the Itacolomi group and even some of the Minas Supergroup is a representative structure in the stability of the slopes of the area (Fontes 2011).

2.2.10 Recent covers

Residual deposits are mainly represented in the area by alluvial bodies located in the north of the study area, along the slopes of the Ouro Preto's hill. Recent debris deposits are represented by canga, cementless ferruginous debris, laterites, and colluvial soils; they have greater spatial distribution in the study area's southwest. Lateritic deposits that are mainly in the plateaus partially cover the formations of the region (Ferreira 2018; CPRM 2016).

CHAPTER 3

SUSCEPTIBILITY

3.1 INTRODUCTION

Susceptibility is the predisposition to the occurrence of phenomena given the characteristics of a given area (Guzzetti *et al.* 2006; Sobreira & Souza 2012). In the context of studies of gravitational mass movements, the analysis of susceptibility is referred to as the study of prediction of unstable areas (Tominaga 2007; Barella 2016). Therefore, it is related to the natural potential of an area to trigger geodynamic events based on the characteristics of the physical environment, although the consequences of the events are disregarded in the analysis (Sobreira & Souza 2012; Barella 2016). There are several definitions given to the term in the context of mass gravitational movements, some of them are shown in Table 3.1.

Table 3.1 - Concepts of susceptibility. Adapted from Corteletti (2017).

Autor	Definition of Susceptibility
Zuquette (1993)	The possibility of a landslide occurring in an area based on terrain conditions. Susceptibility does not explicitly consider the probability of occurrence, which also depends on the recurrence of triggering factors, such as precipitations or earthquakes.
Fell (1994)	It refers to the possibility of a landslide occurrence in an area based on terrain conditions. Susceptibility does not explicitly consider the probability of occurrence, which also depends on the recurrence of trigger factors, such as precipitations or earthquakes.
Soeters & van Westen (1996)	The propensity of a given area to be affected by a (certain type) of landslide, based solely on terrain conditions. It does not give the probability of occurrence of the phenomena.

ISSMGE TC32 (2004) - Glossary of Risk Assessment Terms	It involves the classification of an area (or volume and spatial distribution) and its potential for landslides. It can also include a description of scattering distance, speed, and intensity of the occurred or potential landslide.
Zêzere *et al.* (2005)	The spatial probability of occurrence of a given phenomenon in an area considering the conditioning factors existing on the ground, regardless of its recurrence period; that is, the susceptibility reflects a spatial but not a temporal probability.
AGS (2007) - Australian Geomechanics Society	The quantitative or qualitative assessment of classification, volume (or area), and spatial distribution of occurred or potential landslides. Susceptibility may also include a description of the speed and intensity of existing or potential landslides.
USGS (2008) - States Geological Survey	The possibility that a landslide will occur in an area based on terrain conditions. Susceptibility does not explicitly consider the probability of occurrence, which also depends on the recurrence of trigger factors, such as precipitations or earthquakes.

3.2 LANDSLIDE SUSCEPTIBILITY MAPPING

The landslide susceptibility mapping provides spatial predictability of the occurrence of one or more geodynamic events, showing areas with greater or lesser ability to host these phenomena regardless of temporal probabilities (Barella 2016). The maps are developed at various scales and their product can guide decision-making by public agencies, such as directing detailed studies. Barredo *et al.* (2000) indicate average scales between 1:25,000 and 1:50,000 for the application of statistical

susceptibility methods, while Julião *et al.* (2009) recommend scales ranging from 1:10,000 to 1:25,000. In France, the standard scale adopted is 1:10,000 (Thiery *et al.* 2007). In Brazil, the susceptibility maps which use a mixture of qualitative and quantitative methods are mostly developed on scales ranging from 1:25,000 to 1:50,000 (CPRM 2016).

The methodologies applied to the susceptibility mapping can be classified into qualitative or quantitative and branched into two forms of analysis, as shown in Figure 3.1 (Soeters & van Westen 1996; Aleotty & Chowdury 1999):

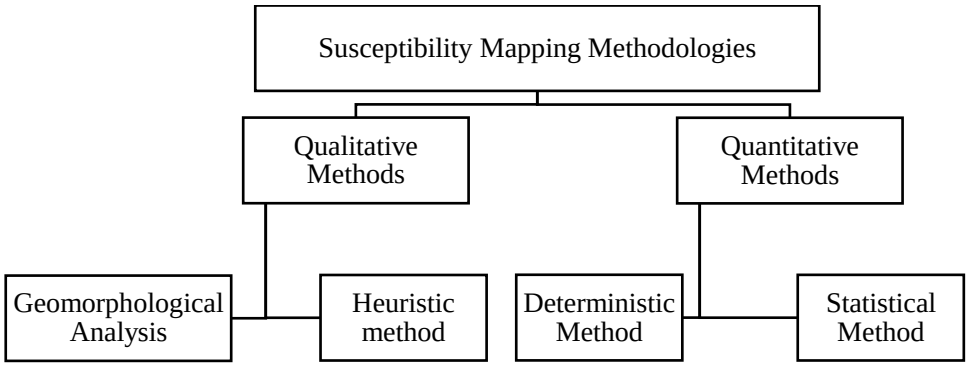

Figure 3.1 - Classification of susceptibility mapping methodologies. Adapted from Soeters & van Westen (1996) and Aleotty & Chowdury (1999).

3.3 QUALITATIVE METHODS

Due to the high subjectivity of qualitative methods, the robustness of susceptibility models produced is related to the experience of the professional in charge. The input data is generally derived from fieldwork and photointerpretation (Aleotty & Chowdury 1999; Barella 2016; Guzzetti *et al.* 1999; Rosa 2018; Soeters & van Westen 1996; Xavier 2018). The procedures applied to this methodology can be classified into two major groups: Geomorphological Analysis and Heuristic Method.

3.3.1 Geomorphological Analysis

The geomorphological analysis is the definition of susceptibility classes in the fieldwork. Although its application is simple and objective, it presents enormous subjectivity (Soeters & van Westen 1996; Guzzetti *et al.* 1999). This methodology has been applied since the 1970s due to the ease of data acquisition, the possibility of application at different scales, and the lack of specific software (Aleotti & Chowdhury 1999; Xavier 2018). However, with the advent of map algebra and the

popularization of computers and software that operate using Geographic Information Systems, this technique has been replaced by less toilsome techniques.

3.3.2 Heuristic Method

The heuristic method consists of assigning weights to predefined cartographic bases followed by map algebra. Although subjective, this methodology is an indirect approach. The product will be conditioned to the weight given to each combined parameter (Guzzetti *et al.* 1999; Fernandes *et al.* 2001). Due to the subjectivity of the weights attributed to the parameters, in a detailed scale, some unacceptable generalizations can occur; therefore, less detailed scales (ranging from 1:100,000 to 1:25,000) are recommended for the application of this method (Barella 2016).

3.4 QUANTITATIVE METHODS

Quantitative methods were developed to decrease the professional's intervention throughout the process; thus, errors of interpretation attributed to the professional's experience are minimized. The procedures applied to this methodology can be classified into two major groups: Deterministic Methods and Statistical Methods.

3.4.1 Deterministic Methods

Deterministic methods are based on numerical models derived from physical properties related to the studied process. The most applied types of analysis in this method are: (i) Limit Equilibrium Method, (ii) Finite Element Method, and (iii) Boundary Element Method. The main outcome of a deterministic analysis in slope stability is the safety factor, which can be performed in two or three dimensions. The needed parameters to run these analyses are mainly dependent on the chosen failure criteria and drainage conditions. Deterministic techniques are correctly applied on a high-detail scale (Gomes *et al.* 2005) given the great variability of parameters according to location, depth, layer, geological structures, or even the load history. In embankments, the result of a deterministic analysis guides mainly in determining the application of support systems as well as determining the face angle of the embankments and berm sizes. The application sectors are diverse, exemplified: mining and enterprise. For the creation of a susceptibility map based on deterministic methods, Aleotti & Chowdhury (1999) recommend individual analysis per slope and later compilation of the results spatially. Some specific models can be applied for the analysis of landslides in large areas, with

emphasis on the SHALSTAB (Montgomery & Dietrich 1994), SINMAP (Pack *et al.* 1998), and TRIGRS (Baum *et al.* 2002) models.

3.4.2 Statistical Methods

Statistical methods are based on the principle that the same parameters that influenced the occurrence of landslides in the past, will influence new events in the future (Aleotti & Chowdhury 1999; Guzzetti *et al.* 1999; Fell *et al.* 2008). These methods generate indirect and quantitative models that establish spatial correlations between events and instability parameters (Guzzetti *et al.* 1999). Thus, they promote impersonality in assigning weight to predisposing factors. Furthermore, the possibility of validating the importance of each conditioning factor and the susceptibility model itself adds robustness to the models produced (Pereira, 2009; Piedade, 2009). However, the statistical approach does not completely remove the subjectivity of the susceptibility models since the choice of parameters and the form of cartographic representation of the inventories is made by the professional in charge.

Despite the robustness of statistical methods, Thiery *et al.* (2007) and van Westen *et al.* (2003) state that the independence of the prediction variables does not match, in most cases, the reality of the terrain. However, once the combination of the dependent parameters is performed to produce an independent factor, this disadvantage of statistical approaches can be avoided. Another disadvantage is the application of the same integration and hierarchy of predisposing factors across the study area, a fact that also does not match the reality of most terrains (Barella 2016; Xavier 2018).

Statistical analysis is widely applied in susceptibility studies and models with high predictive capacity are often obtained (Reichenbach *et al.* 2018). Soeters & van Westen (1996) indicate the use of this approach on a scale of 1:25,000; however, van Westen (2000) recommends the use on a scale of up to 1:50,000. In these susceptibility studies, multivariate and bivariate analyses are employed.

Multivariate analysis adds to the construction of susceptibility models the interaction between predisposing factors (Suzen & Doyuran 2004). For landslides, this methodology was applied firstly in the zoning of Italy (Soeters & van Westen 1996); however, it was already widespread in studies of mineral and oil exploration (Carrara 1993). The most applied models end with Discriminant Analysis, Linear Regression, Logistic Regression, and Neural Networks. According to Barella (2016) for the application of multivariate analysis in the landslide susceptibility mapping, the following steps should be followed: (1) selection and mapping of the conditioning factors and elaboration of a map of landslide inventory in the study area; (2) screening of samples affected and not affected by landslides using the features cataloged in the inventory; (3) overlapping the predisposing parameter maps with the defined samples; (4) based on binary sampling (stable/unstable), elaborate a presence/absence

relationship for each class of each parameter; (5) application of a multivariate statistical model; (6) categorization of susceptibility classes, based on the reclassification of land units.

In bivariate analysis, the weighting value is obtained statistically by overlapping conditioning factors and the inventory of landslides; thus, the weighting is performed by calculating the landslide density for each class of each parameter. The bivariate methodology can be summarized according to the stages (Aleotti & Chowdhury 1999): (1) choice of parameters that condition the events; (2) subdivision of the chosen parameters in classes; (3) preparation of an inventory map; (4) overlapping the parameter maps with the inventory map; (5) assignment of the weights of importance for each class of each parameter according to the landslide density calculation; (6) integration of the cartographic bases of the parameters with subsequent integration of the susceptibility classes. To calculate the weighting values, several bivariate methodologies are used, the most well-known ones are Likelihood ratio, Informational Value and Evidence Weights, and Favorability Functions (Corominas *et al.* 2014).

CHAPTER 4

METHODOLOGY

4.1 LITERATURE REVIEW

Texts and articles with themes related to landslide susceptibility mapping, local and regional geology as well as landslide volume assessment were used as a reference in this work.

4.2 LANDSLIDE INVENTORY

The preparation of a landslide inventory involved the aerial assessment of 57 slide features using a rotating wing Unmanned Aerial Vehicle (UAV) (DJI Phantom 3 Advanced). Rotating wing UAVs feature stability, low cost and, in general, quality pictures, and are easily operated in hard-to-reach regions (Akturk & Altunel 2019). Because a highly reliable landslide inventory was desired, only those features that preserved volumetric proportions similar to the actual volume of the event were catalogued. Scars with advanced erosion, resloping or covered by dense vegetation were not considered.

The images obtained with the UAV were collected with the help of the DroneDeploy software. The following parameters were considered in the survey: (i) landslide features were positioned in the centre of the flight paths to minimize edge errors; (ii) the average flight height was 120 meters above ground level. Thus, the superimposed images had more points of similarity for processing. Given the flight height and the characteristics of the UAV digital camera, the average resolution of the images was 5.1 cm/pixel; (iii) the average flight speed varied according to the available luminosity during mapping, ranging between 9 m/s on cloudy days and 11 m/s on sunny days; and (iv) the average overlap of images was 80% (vertical) and 80% (horizontal). Images were processed with the Agisoft PhotoScan software, allowing the digital terrain model (DTM) (Figure 1.2A), orthophotos (Figure 1.2B), and displaced volume from the rupture zone to be calculated from the landslide's features. On average, the error along the X, Y, Z axes was 1.1 m, 2.6 m and 0.5 m, respectively.

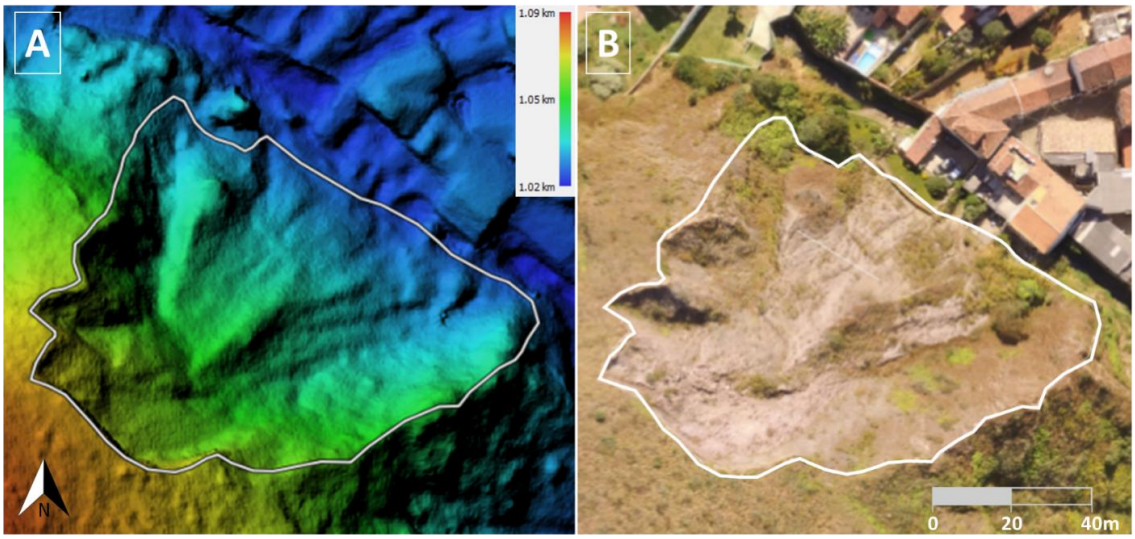

Figure 4.1 - Example of the information obtained from the processing of the airborne data. (A) DTM, (B) Orthophoto.

The polygonal cartographic delimitation of landslide features was performed in ArcGIS 10.3 software from the orthomosaics produced. For each vectorized feature, the area of the rupture zone was calculated. Thus, the inventory of landslides produced presents, besides the spatial location of the events, alphanumeric information regarding the area of the rupture zone and the volume mobilized. From these data, a regression curve was generated (Rice *et al.* 1969; Innes 1983; Guthrie & Evans 2004; Korup 2005; Imaizumi & Sidle 2007; Imaizumi *et al.* 2007; Guzzetti *et al.* 2006, 2009), allowing the future determination of the volume of any landslide that occurs in the region from determination of its area.

4.3 LANDSLIDE CONDITIONING FACTORS

The choice of landslide conditioning factors for the construction of statistical susceptibility models is dependent on the characteristics of the study area and data availability, and relevant factors in one area may not be relevant in another (Shahabi & Hashim 2015). However, some landslide conditioning factors, including slope aspect, lithology, soils, land use and land cover, among others, are constantly found in a variety of studies (Corominas *et al.* 2014; Achour *et al.* 2017; Pham *et al.* 2018; Barella *et al.* 2019; Xiao *et al.* 2020). Pereira *et al.* (2012) demonstrated that robust landslide susceptibility models can be obtained using few parameters, which contributes to a greater conditional independence of the models. The following factors were chosen for the study area: lithological units, slope angle, geomorphological units, slope aspect, and land use.

Slope angle (Figure 1.3B) is one of the most important parameters used in the analysis of gravitational mass movements (Corominas *et al.* 2014; Ba *et al.* 2017; Schlögel *et al.* 2018; Pham *et al.* 2018; Aditian *et al.* 2018; Amato *et al.* 2019; Li *et al.* 2019; Nohani *et al.* 2019). In the present study area, inclination ranged from 0° to 65.3°, using classes of 5° amplitude. Slope aspect (Figure 1.3D) was classified based on azimuth in cardinal and collateral points. This parameter influences local soil moisture content, weathering and vegetation growth (Camilo *et al.* 2017; Shirzadi *et al.* 2017; Wang *et al.* 2017; Zêzere *et al.* 2017; Sun *et al.* 2020; Chen & Li 2020), in addition to correlating with the containment of slope discontinuities.

The geological map of the study area (Lobato *et al.* 2005) was regrouped in lithological units based on stability inferences (Varnes *et al.* 1984), not necessarily respecting the stratigraphic division defined by Dorr (1969). Thus, the lithology was divided into six lithological units (Figure 1.3A) grouping rock types with similar geotechnical behaviour: phyllites (LUn 1); banded iron formation (BIF) (LUn 2); quartzite (LUn 3); schist (LUn 4); dyke (LUn 5); and dolomite (LUn 6).

The Geomorphological Units (GU) (Figure 1.3C) is often associated with the occurrence of landslides (Süzen & Doyuran 2004; Bălteanu *et al.* 2010; Chen *et al.* 2016; Aditian *et al.* 2018). Geomorphological Units were divided into 5 units (Ponçano *et al.* 1979): hilltop relief (GU 1), hilly relief with smooth slopes (GU 2), hilly relief (GU 3), hill relief (GU 4) and mountain relief (GU 5). Land use is another important landslide conditioning factor, as it is related to human interference, which may affect slope stability (Pereira *et al.* 2012; Zêzere *et al.* 2017; Pourghasemi *et al.* 2018; Schlögel *et al.* 2018; Nohani *et al.* 2019; Sun *et al.* 2020; Chen & Li 2020). This parameter was divided into 11 classes (Figure 1.3E): industrial and/or commercial area (LUs 1), university centre (LUs 2), lagoon (LUs 3), mining (LUs 4), urban occupation of high (LUs 5), normal (LUs 6) and low (LUs 7) construction patterns, exposed rock (LUs 8), exposed soil (LUs 9), and high (LUs 10) and low (LUs 11) vegetation cover.

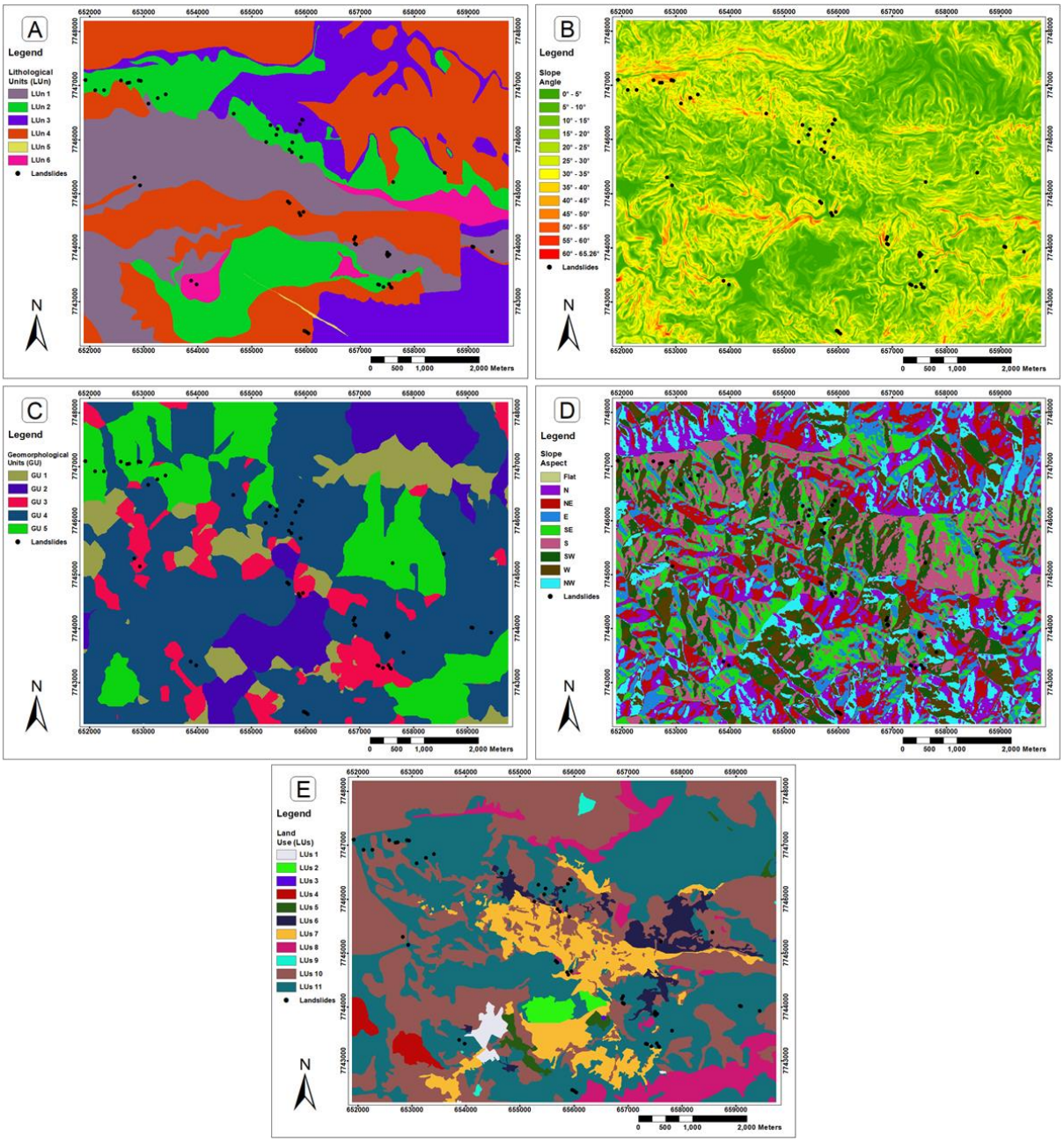

Figure 4.2 - Conditioning factors used in the construction of susceptibility models. (A) Lithological Units, (B) Slope Angle, (C) Geomorphological Units, (D) Slope Aspect, and (E) Land Use. These images are in higher resolution in the appendix.

4.4 LANDSLIDE SUSCEPTIBILITY MODELS

Landslide susceptibility models are created with different combinations of parameters to determine their interrelationship with the landslide's distribution (Pardeshi *et al.* 2013). Therefore, it is important to use devices to produce autonomous landslide subgroups (training and test samples) to

assess the quality of the produced models (Chung & Fabbri 2003). The inventory of landslides was randomly divided 50 times between the training and test groups, with a fixed the proportion 70%/30% in all divisions, respectively. A designation of 2/3 of the data to compose the training set and reserve 1/3 to structure the validation set (Kohavi 1996) has been commonly applied in previous studies.

Using the volumetric data of the landslide features as a metric to characterise the magnitude of past events, three divisions were selected to be statistically modelled among the 50 divisions of the inventory. There were: (i) balanced division (training and test groups with the most similar volumes found); (ii) unbalanced division 1 (predominance of the largest volumes in the test group); and (iii) unbalanced division 2 (predominance of the largest volumes in the training group). Table 1.1 presents the mean, the largest and the smallest volume, and area of the landslides of the three selected divisions.

Table 4.1 - Inventory shares between the training (70%) and test (30%) groups as a function of the volume mobilized in the mapped landslides features.

	Volume (m^3)		**Area (m^2)**	
	Training	**Test**	**Training**	**Test**
Balanced (smaller difference between training and test volumes)				
Minimum	1.5	22.3	4.6	44.9
Average	27710.4	31785.4	2952.4	4112.3
Maximum	768657.1	476542.7	51681.0	50879.8
Unbalanced 1 (test containing the largest volumes)				
Minimum	1.5	35.9	4.6	47.3
Average	5962.0	82958.1	1527.9	7463.9
Maximum	107091.9	768657.1	17416.0	51681.0
Unbalanced 2 (training containing the largest volumes)				
Minimum	1.5	4.0	4.6	9.8
Average	40507.4	1674.9	4469.9	541.6
Maximum	768657.1	14239.8	51681.0	3713.3

Based on the three partitions selected from the polygonal format inventory, another five point inventories were built based on the same mapped landslide features, one with the allocation of a point vector in the centre of mass of the landslides and another four with random points distributed inside the features (Figure 1.4). Thus, the landslides were represented in the form of polygon and points, and the susceptibility models developed took into consideration the six adopted cartographic representations (polygon, point in the centre of mass of the slide features, and random points distributed inside the slide features). 18 susceptibility models were produced from the combination of the three divisions selected among the training and test groups and the six cartographic representations

of the landslide inventory. The assessment of random point vector dispersion was measured by the Euclidean distance of the points in relation to the landslides' centres of mass and by the predominant spatial location within the mapped slide features (NW, NE, SW and SE quadrants).

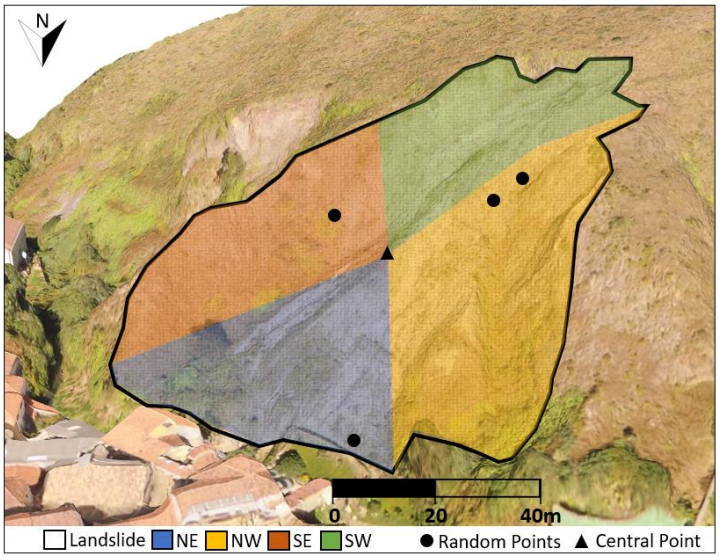

Figure 4.3 - Example of the distribution of points inside the landslide features

Construction of the models was done using the informative value equation (1), which is a simple, intelligible and effective bivariate statistical approach, widely used in the construction of landslide susceptibility maps (Zêzere 2002; Pereira *et al.* 2012; Pardeshi *et al.* 2013; Oliveira *et al.* 2015; Chen *et al.* 2016; Pereira *et al.* 2017; Du *et al.* 2017; Ba *et al.* 2017; Sharma & Mahajan 2018; Banerjee *et al.* 2018; Li *et al.* 2019):

$$VI_i = ln\left[\frac{S_i/N_i}{S/N}\right] \quad (1)$$

where, VI_i= Informative Value of variable *i* (parameter class); S_i= Number of plot units of variable i with landslides; N_i = Number of plot units of variable i; S = Total number of plot units with landslides; N = Total number of plot units of study area. When VI_i is positive, the variable i is relevant

to explain the spatial distribution of the landslide. The degree of importance of the variable increases with increasing score.

After calculating the VI for each class, of each conditioning factor, rasters derived from these values were superimposed in a GIS environment to obtain the Landslide Susceptibility Index (LSI). The LSI was calculated from the sum of the informative value of the pixels of the conditioning factors equation (2).

$$LSI_j = \sum_{i=1}^{M} X_{ji} \times VI_i \quad (2)$$

where, X_{ij}=1 if variable i exists in pixel j and 0 if variable i does not exist in pixel j; M = number of variables considered.

Validation of the susceptibility models was performed by calculating the area under the success rate curve (Chung & Fabbri 1999, 2003). The success curve measures the degree of fit of the model to the training inventory, while the prediction curve measures the fit to the test inventory (Zêzere *et al.* 2017). Thus, this curve evaluates the model's ability to predict new landslides. In both cases, the steeper the curve, the higher the area under the curve (AUC) and the better the model's ability to describe the distribution of a landslide (Chung & Fabbri 2003; Blahut *et al.* 2010; Corominas & Mavrouli 2011).

As the model is applied to the training data, it is expected that the success curve will always be higher than the prediction curve (Chung & Fabbri 2003). However, this pattern is not always observed. Thus, to produce more conservative susceptibility models for the study area, the worst performance between success and prediction rates should be classified. This decision tends to produce models with larger areas of high susceptibility but is safer when used to predict future landslides.

Of the 18 models produced, only two models from each of the divisions adopted among the training and test subgroups (balanced, unbalanced 1, and unbalanced 2) were classified. These models present the most discrepant validation results obtained in the present study (the best and worst models of each division). For the classification, the following predictive abilities to find future landslides were adopted: 80% (high susceptibility class), 15% (medium susceptibility class), and 5% (low susceptibility class). The smallest area below the curve between the success and prediction curves was adopted in this stage. These models were compared with the objective of evaluating the lack of spatial

agreement produced as a function of the cartographic representation adopted for the dependent variables.

All the methodological steps developed, and data used, are presented in a simplified flowchart (Figure 1.5).

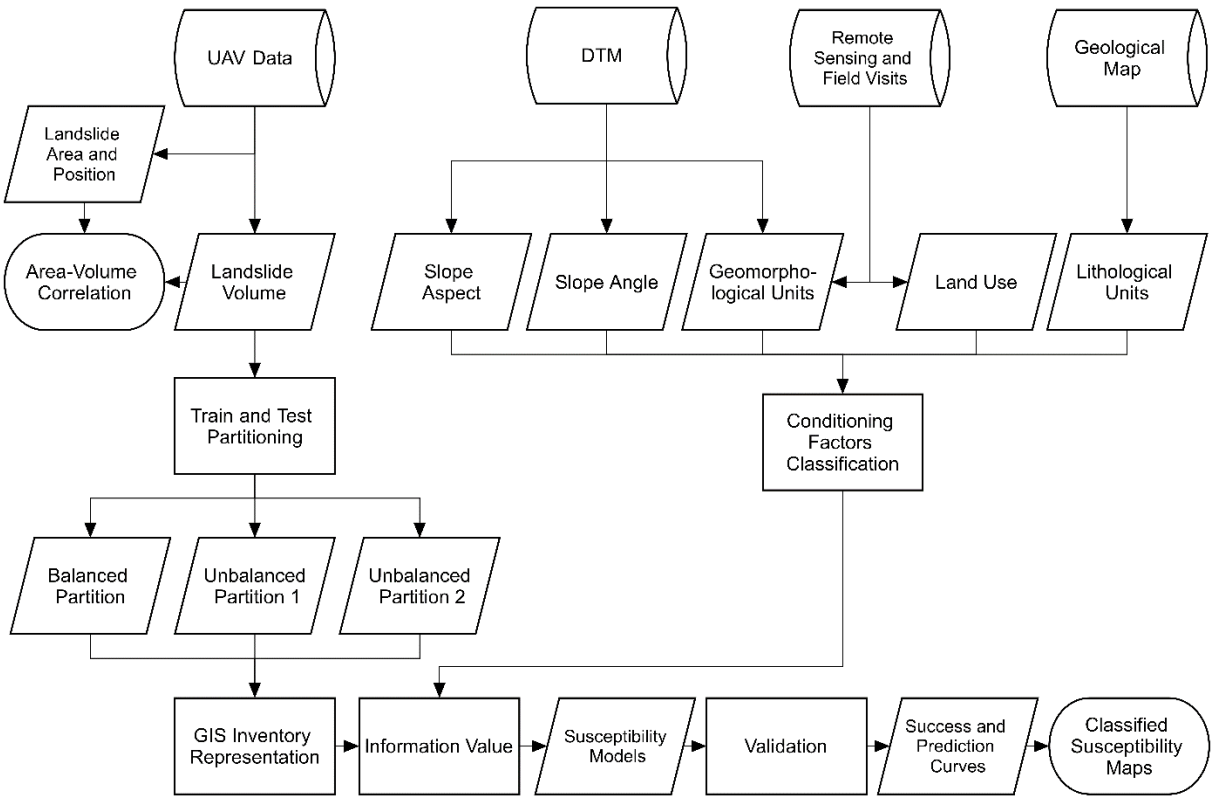

Figure 4.4 - Simplified flowchart of developed methodological activities.

CHAPTER 5

RESULTS AND DISCUSSION

5.1 INTRODUCTION

If conditioning factors have different degrees of influence on landslides of small and large magnitude (Constantin *et al.* 2011; Zizioli *et al.* 2013; Nhu *et al.* 2020), the volumes and areas of the listed landslides features were determined, then a statistical correlation between area and volume for the study area was established (Figure 4.1). The correlation calculated equation (3) was highly significant ($R^2 = 0.9687$) and can be applied to any area with similar geological and geomorphological features to identify the volume of landslides with area ranging from 4.6 to 51.681,0 m²:

$$V = 0.1954 \times A^{1.3623} \quad (3)$$

where, V = Volume of landslide and A = area of the landslide feature.

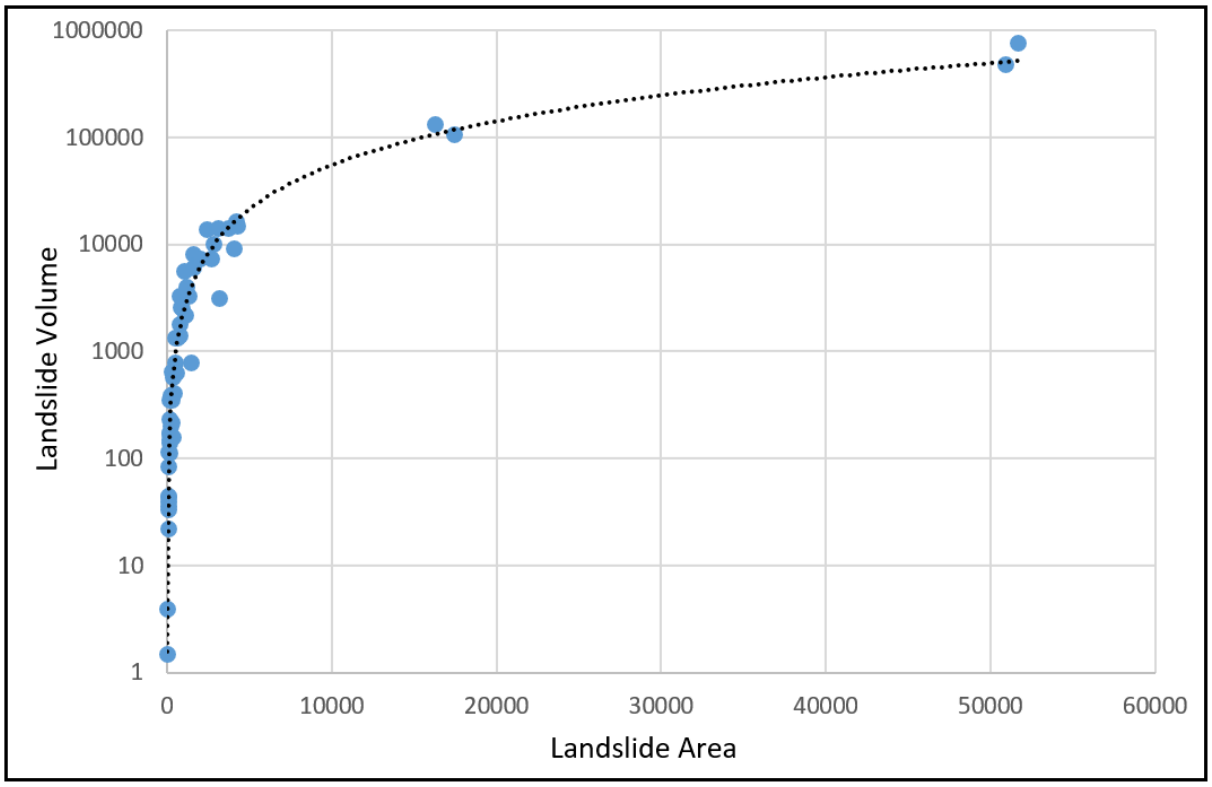

Figure 5.1 - Correlation of the area and volume of landslides in the study area

5.1.1 Well-balanced Division

When the sample space partition was balanced, the best performance (success and prediction rate curves) was found when the mapping features were polygonal (Table 4.1). The simulation performed with point features located in the centre of mass of the landslides showed a slightly lower performance than some simulations performed with random points distributed within the landslide (M2 and M4). Therefore, the randomness in the distribution of the point features within the landslides' scars did not negatively influence the result.

Table 5.1 - Well-balanced random sample.

Model	Landslide feature	Success-rate curve (training)	Prediction-rate curve (test)
M1	Polygon	0.934	0.961
M2	Centralized point	0.871	0.851
M3	Random point features 1	0.850	0.867
M4	Random point features 2	0.877	0.855
M5	Random point features 3	0.864	0.848
M6	Random point features 4	0.861	0.921

Among the models developed with point cartographic features, the best result was observed in M6. This model presented a similar spatial dispersal of points between the training and test subgroups (Figure 4.2). On average, the points were closer to the centres of mass and their locations were predominantly in the NW and NE quadrants. The worst result was observed in M5. This model presented a more discrepant randomness compared to M6. It showed a higher distance to the centres of mass in the training subgroup data, with a slightly predominant location in the NW and NE quadrants. In contrast, data from the test subgroup of this model showed a reduction in distance to centres of mass and were preferentially located in the SE quadrant. M3 presented a validation result very close to M5, but with an inversion in the results of the areas below the success and prediction curve. The distance to the centres of mass of M3 and M5 was also similar in the training and test groups. In the training subgroups, M3 exhibited a higher concentration of points in the SW quadrant, while M5 exhibited a higher concentration in the NE quadrant. However, in the test subgroups, M3 presented a balanced dispersion of points in the quadrants, while M5 points were concentrated in the SE quadrant.

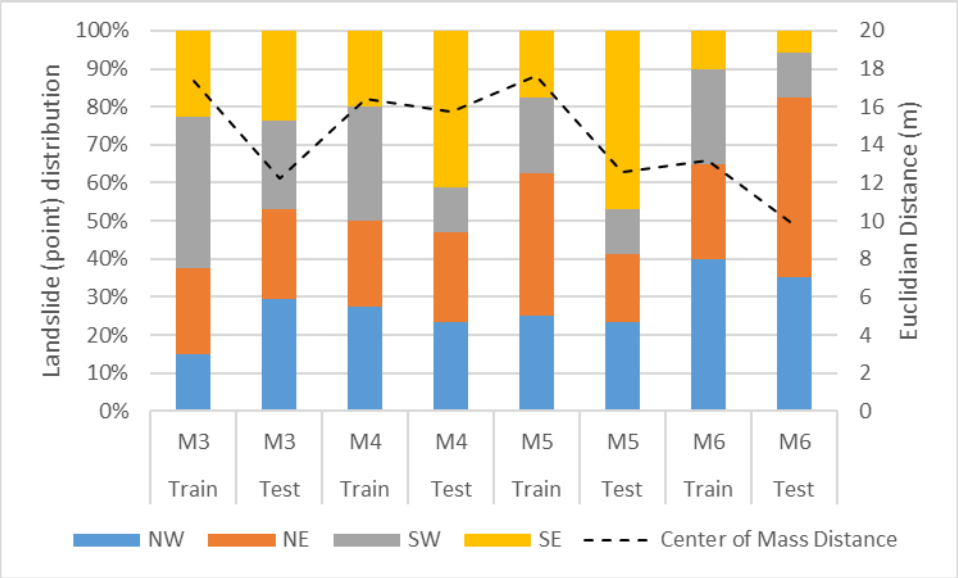

Figure 5.2 - Spatial distribution of the random points of the balanced partition.

Analysis of the influence of conditioning factors on the development of the investigated landslides according to the adopted cartographic representation revealed variations in the scores, although common trends were observed among all susceptibility models produced. For the evaluation of the scores, models with higher and lower robustness (M1 and M5), based on the AUC values are highlighted. The classes of the most influential conditioning factors were maintained, except for geomorphological units. Another large discrepancy was also found in the slope aspect.

The model that adopted polygonal cartographic representation (M1) was influenced by the following conditioning factors: quartzite (IV = 1.294) and dolomite (IV = 0.126) lithological units; slope ranging from 25° to 60°, with the highest and lowest scores found in the 50°-55° (IV = 3.155) and 25°-30° (IV = 0.083) ranges, respectively; geomorphologic unit of mountainous relief (IV = 1.040), which contained scars of large volume in the training subgroup; slopes oriented to S (IV = 0.768) and SO (IV = 1.100); and land use characterised as low vegetation (IV = 0.569). In turn, the model that adopted the random point representation 3 (M5) was influenced by the following conditioning factors: lithological units of quartzite (IV = 0.718), dolomite (IV = 0.461), and phyllite (IV = 0.034); slope ranging from 25° to 55°, with the highest and lowest scores in the 50°-55° (IV = 2.838) and 25°-30° (IV = 0.790) ranges, respectively; hilly (IV = 0.558) and hill geomorphological units (IV = 0.276); slopes oriented to N (IV = 0.116), NE (IV = 0.195), E (IV = 0.015), SO (IV = 0.526), and O (IV = 0.233); and land use characterised as low vegetation (IV = 0.479). Figure 4.3 presents the classified susceptibility maps for these models.

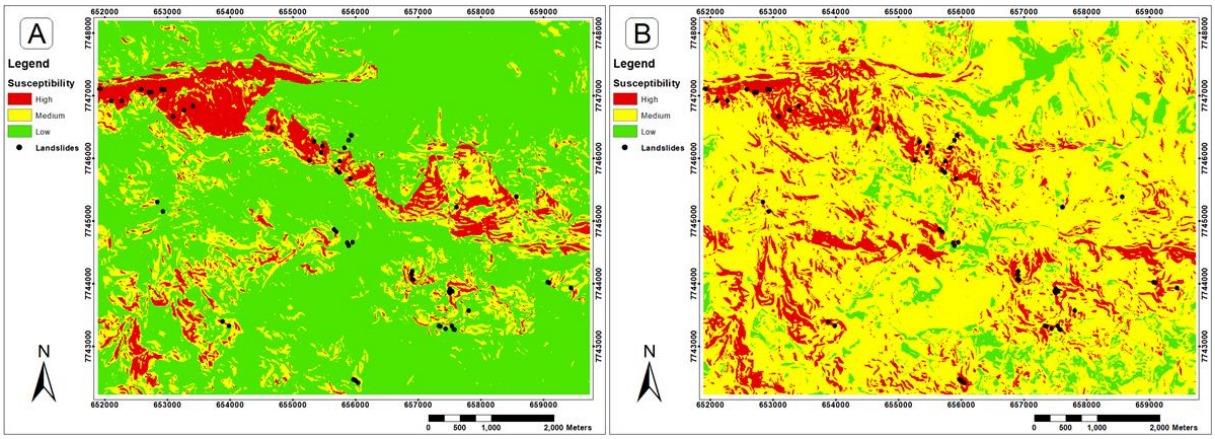

Figure 5.3 - Classified susceptibility maps for models that used (A) polygonal (M1) and (B) random spot 3 (M5) representation. These images are in higher resolution in the appendix.

The susceptibility map classified from the polygonal features training subgroup has high, medium and low susceptibility classes accounting for 9.92%, 18.25% and 71.83% of the study area, respectively (Figure 4.3A). The map classified from the randomized point representation of test subgroup 3 (M5) has high, medium and low susceptibility classes, accounting for 13.90%, 77.11% and 8.98% of the territory, respectively (Figure 4.3B). The maps of these models have a spatial discrepancy of 71.83% among the adopted susceptibility classes. There was an increase in the area of high and medium susceptibility classes compared to M1 to M5.

5.1.2 Unbalanced Division 1

Unbalanced division 1, which contained a predominance of landslides of great magnitude in the test subgroup, also exhibited polygonal representation as the best result. In this uneven distribution of the sample space between the training and test groups, the random distribution of the point features negatively influenced the results. The validation results of M9, M10, M11 and M12 models were inferior to the model developed with points located in the centres of mass of the landslide (Table 4.2). All models produced with this unbalanced partition showed, on average, a similar distance from the centres of mass for the data of the training subgroup, due to the small area of landslides. Among the susceptibility models produced with random points, M10 and M12 models exhibited the worst and best performance, respectively.

Table 5.2 - Unbalanced 1 random sample.

Model	Landslide feature	Success-rate curve (training)	Prediction-rate curve (test)
M7	Polygon features	0.914	0.925
M8	Centralized point feature	0.881	0.878
M9	Random point features 1	0.876	0.818
M10	Random point features 2	0.846	0.785
M11	Random point features 3	0.854	0.855
M12	Random point features 4	0.902	0.859

The M10 points were closer to the centres of mass than the other models, both for the training and the test subgroups. The training subgroup exhibited a more dispersed distribution of points between the 4 quadrants (NW, NE, SW and SE) and the test subgroup exhibited a concentrated location in the SE and SW quadrants (Figure 4.4). M12 showed a distance from the centre of mass very similar to M9, both for training and test subgroup's data. However, while the points in M12 were located predominantly in the SW and SE quadrants, for both subgroups, M9 exhibited points located predominantly in the NW and NE quadrants in the training subgroup and SW and SE in the test subgroup. M11 exhibited a test subgroup with points more distant from the centres of mass, located primarily in the NE and NW quadrants. In contrast, the training subgroup of the same model exhibited points closer to the centres of mass and located predominantly in the SE and SW quadrants. Therefore, the randomness in the distribution of point features within the landslides appeared to influence the result in a non-standard way, that is, sometimes points distributed in a more random way (less concentrated in a specific portion of the landslide) produce more robust results.

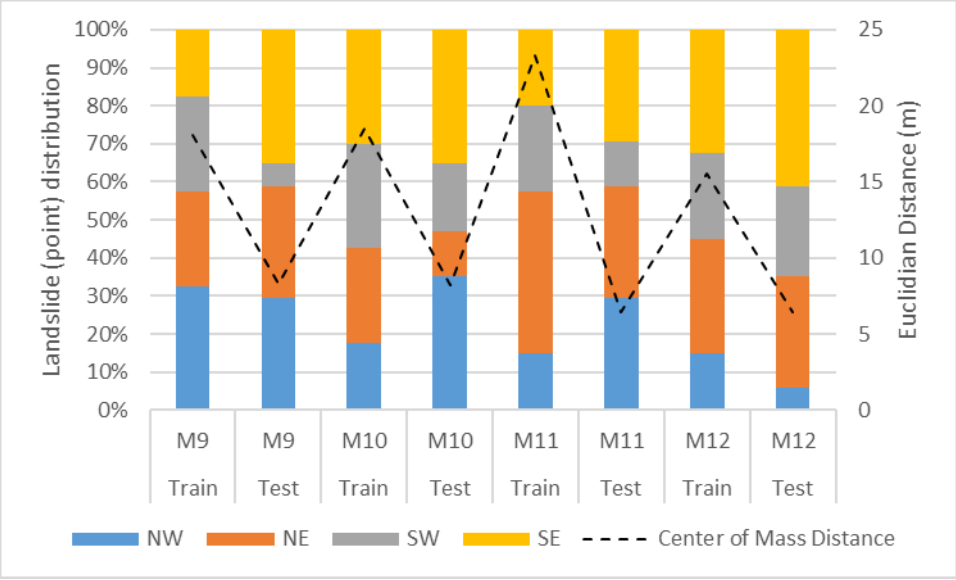

Figure 5.4 - Spatial distribution of random points of the unbalanced partition 1.

The model that adopted polygonal cartographic representation (M7) was influenced by the following conditioning factors: quartzite (IV = 0.826), dolomite (IV = 0.719) and phyllite (IV = 0.442) lithological units; slope ranging from 25° to 55°, with the highest and lowest scores in the ranges 50°-55° (IV = 2.710) and 25°-30° (IV = 0.405), respectively; hill relief geomorphologic unit (IV = 0.405); slopes oriented to S (IV = 0.279) and SO (IV = 1.307); and land use characterised as low vegetation (IV = 0.446) and urban occupation of medium construction pattern (IV = 0.036). In turn, the model that adopted the random point representation 2 (M10) was influenced by the following conditioning factors: quartzite lithological units (IV = 0.718); slope ranging from 25° to 40°, with the highest and lowest scores in the ranges 35°-40° (IV = 1.856) and 25°-30° (IV = 0.877), respectively; hilly geomorphological units (IV = 0.713) and hills (IV = 0.311); slopes oriented to NE (IV = 0.446), SE (IV = 0.019), S (IV = 0.152), SO (IV = 0.749) and O (IV = 0.010); and land use characterised as low vegetation (IV = 0.479). Figure 4.5 presents the classified susceptibility maps for the most discrepant models in this division of dependent variables (polygonal and random spot representation 2 (M10)).

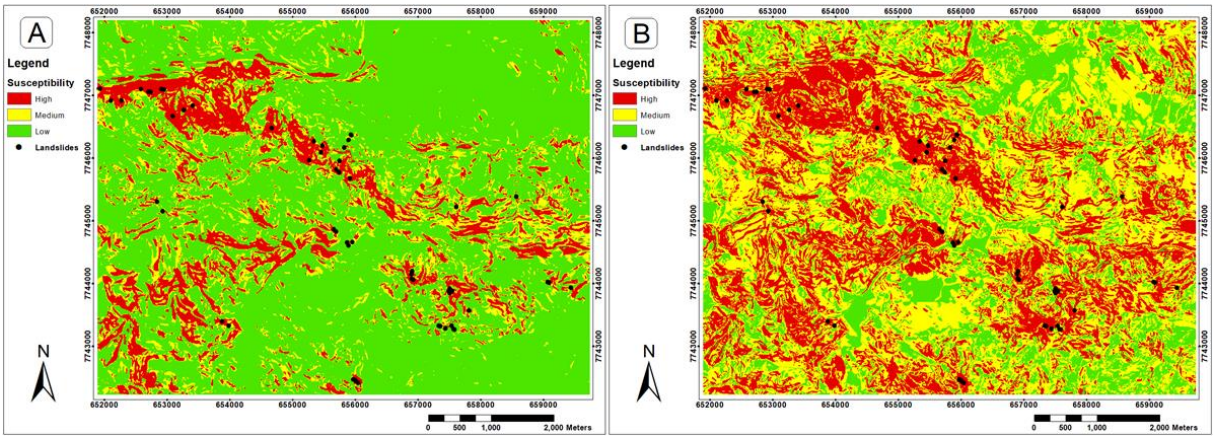

Figure 5.5 - Classified susceptibility maps for models that used (A) polygonal (M7) and (B) random spot representation 2 (M10). These images are in higher resolution in the appendix.

The susceptibility map classified from the polygonal features test subgroup has high, medium and low susceptibility classes accounting for14.41%, 14.11% and 71.48% of the study area, respectively (Figure 4.5A). The map classified from the randomized point representation test subgroup 2 (M10) has high, medium and low susceptibility classes accounting for 31.33%, 45.10% and 23.57% of the territory, respectively (Figure 4.5B). The maps of these models have a spatial discrepancy of 59.25% among the adopted susceptibility classes. There was an increase in the area of the high and medium susceptibility classes compared to M7 to M10.

5.1.3 Unbalanced Division 2

The last division of the data between the training and test subgroups, called unbalanced 2, prioritized the major landslide features in the training subgroup. This approach produced, for the polygonal landslide inventory, the best success rate, a result that was not followed by the prediction rate (Table 4.3), which was lower than all other models produced, except for M16, which was developed with random points. In this division of the dependent variables between the training and test subgroups, the different trend was observed compared to the previous divisions, which showed the most robust result in the model produced with polygonal features.

Table 5.3 - Unbalanced 2 random sample.

Model	Landslide feature	Success-rate curve (training)	Prediction-rate curve (test)
M13	Polygon features	0.950	0.807
M14	Centralized point feature	0.873	0.813
M15	Random point features 1	0.883	0.850
M16	Random point features 2	0.873	0.786
M17	Random point features 3	0.839	0.864
M18	Random point features 4	0.872	0.825

As in the unbalanced division 1, the differences observed in the Euclidean distance of the random points (M15, M16, M17 and M18) in the training and test subgroups occurred due to the size of the landslides features in each subgroup. Therefore, the small landslide features positioned the points closer to the centre of mass (test subgroup), while the larger events allowed the dispersion of the points (training subgroup), as shown in Figure 4.6. For this partition of sample space, the best result was in M15 developed with the random point features 1, and the worst result was in M16 developed with the random point features 2. The M15 and M16 models exhibited well distributed points in the training subgroups, with a slight predominance of NW and NE in M15 and SW and SE in M16. The test and training subgroups of M15 exhibited a slight predominance NW and NE, but a decrease of points in the SW quadrant and an increase in the SE quadrant. The test subgroup of M16 exhibited a distribution of points predominantly in the NW and SE quadrants.

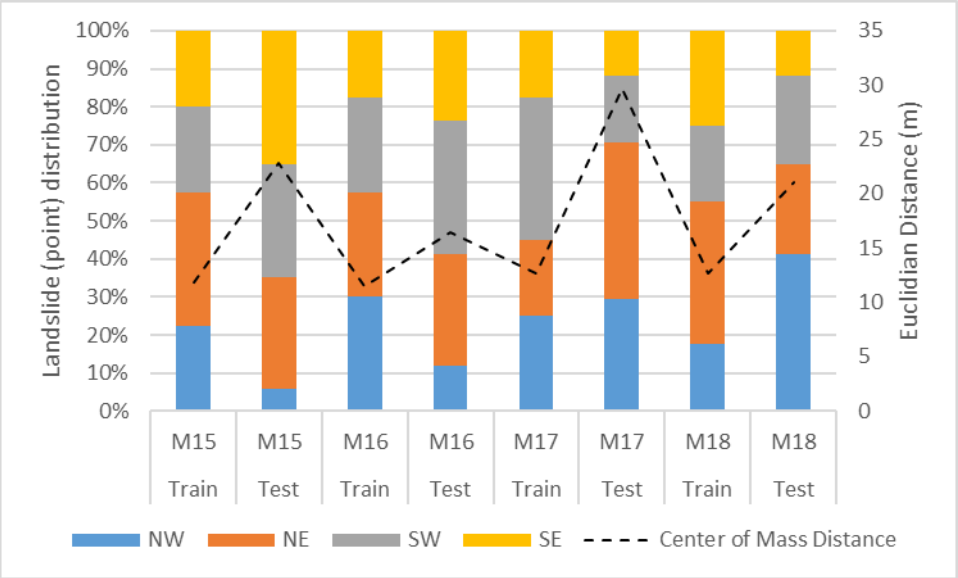

Figure 5.6 - Spatial distribution of random points of the unbalanced partition 2.

Analysis of scores between these models (M15 and M16) revealed that M15 was influenced by the following conditioning factors: lithological units of quartzite (IV = 0.955) and dolomite (IV = 0.461); slope ranging from 25° to 50° with the highest and lowest scores in the ranges 45°-50° (IV = 2.937) and 40°-45° (IV = 0.322), respectively; hilly geomorphological units (IV = 0.713), mountainous relief (IV = 0.219) and hill (IV = 0.121); slopes facing SO (IV = 0.931), S (IV = 0.286) and O (IV = 0.010); and land use characterised as low vegetation (IV = 0.550). The model that adopted the random point representation 2 (M16), with the lowest predictive capacity, was influenced by the following conditioning factors: lithological units of quartzite (IV = 0.955) and dolomite (IV = 0.461); slope ranging from 20° to 45°, with the highest and lowest scores in the ranges 40°-45° (IV = 1.015) and 20°-25° (IV = 0.078), respectively; hilly geomorphological units (IV = 0.558), mountainous relief (IV = 0.219) and hill (IV = 0.162); slopes oriented to NE (IV = 0.328), S (IV = 0.286) and SO (IV = 0.931); and land use characterised as low vegetation (IV = 0.515). Figure 4.7 presents the classified susceptibility maps for models M15 and M16.

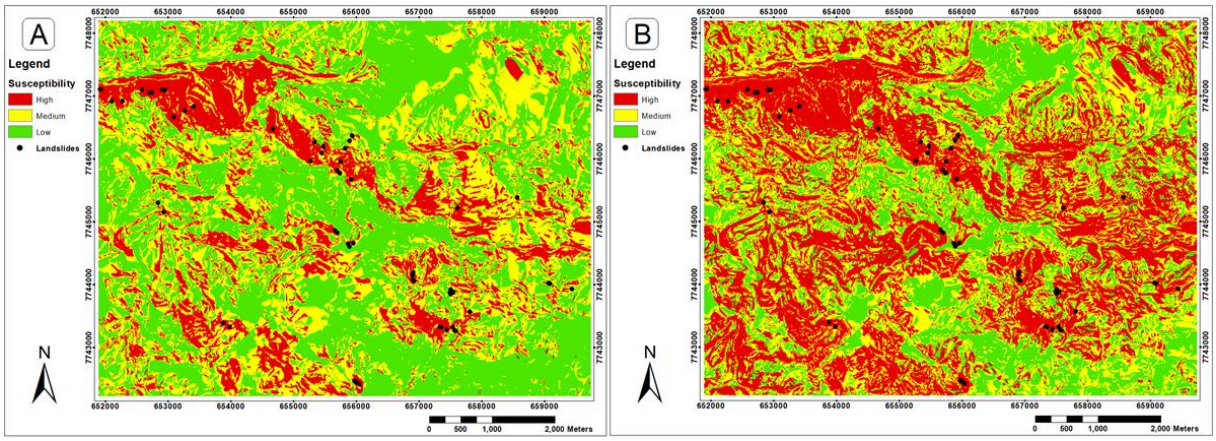

Figure 5.7 - Classified susceptibility maps for the models M15 and M16 that used random point cartographic representation (A) 1 and (B) 2. These images are in higher resolution in the appendix.

The susceptibility map classified from the random point representation 1 test group (M15) has high, medium and low susceptibility classes, accounting for 19.93%, 33.83% and 46.25% of the study area (Figure 4.7A). The map obtained from randomized point representation test group 2 (M16) has high, medium and low susceptibility classes, accounting for 41.89%, 31.74% and 26.37% of the study area, respectively (Figure 4.7B). The maps of these models have a spatial discrepancy of 42.91% among the adopted susceptibility classes. There was an increase in the area of the high susceptibility class compared M15 to M16.

CHAPTER 6

CONCLUSIONS

This study tested, validated and compared different cartographic representations of a landslide inventory for construction of susceptibility models. We also determined the correlation between area and volume for landslides in the investigated region. In general, besides the change in the magnitude of some scores among all the cartographic representations adopted, the change of importance in some classes of the conditioning factors was also identified. The main conclusions are:

1. The correlation between the area and volume of landslide scars had an R^2 close to 1. This indicates the robustness of the exponential curve used and reinforces the application of the derived equation in future volumetric studies in the region.

2. All landslide susceptibility models applied in this study achieved good results, regardless of the cartographic representation adopted to map landslide features. The worst result was a random and point-based cartographic representation and a partition of dependent variables with a predominance of large and deep landslides in the training group. The best result was obtained when a polygonal cartographic representation was used and a balanced partition of the dependent variables (large and deep landslides in both training and test subgroups).

3. There was a tendency for the conditioning factors to vary according to training with different cartographic features (polygon, point in the centre of mass and random point), as well as with small and large landslide features, which influenced the quality of the susceptibility models. Thus, despite the robustness exhibited by two susceptibility models produced with slipped features mapped with polygonal vectors, this study does not allow us to state, categorically, that this cartographic representation was optimal.

4. The distribution of high, medium and low susceptibility classes varied markedly throughout the study area, although the predictive capacity was kept constant in each class (high = 80%, medium = 15% and low = 5%). This spatial discrepancy in the models was produced by the cartographic representations adopted and/or by the partition of the dependent variables between the training and test subgroups.

5. The adoption of different cartographic representations to map the features of landslides in regions that register movements of different magnitudes can interfere in the quality of the application of models and in the spatial arrangement of the susceptibility classes, producing different maps for the same locality.

For future work, it is suggested:

1. Verify if the drone error was relevant for the analysis of the effect of the cartographic representation in the susceptibility models and area-volume regression curve, through the application of ground control points and other methodologies to increase the accuracy of UAV surveys.

2. Incorporate new landslides' features in the area-volume regression curve as in the analysis of the effect of cartographic representation on susceptibility models.

REFERENCES

Achour, Y., Boumezbeur, A., Hadji, R., Chouabbi, A., Cavaleiro, V., Bendaoud, E.A. 2017. Landslide susceptibility mapping using analytic hierarchy process and information value methods along a highway road section in Constantine, Algeria. Arabian Journal of Geosciences 10. https://doi.org/10.1007/s12517-017-2980-6

Aditian, A., Kubota, T., Shinohara, Y. 2018. Comparison of GIS-based landslide susceptibility models using frequency ratio, logistic regression, and artificial neural network in a tertiary region of Ambon, Indonesia. Geomorphology 318:101–111. https://doi.org/10.1016/j.geomorph.2018.06.006

AGS. Practice Note Guidelines for Landslide Risk Management. Australian Geomechanics Society Landslide Taskforce Landslide Zoning Working Group. 2007. Australian Geomechanics 42 (1), 63–114.

Akturk, E., Altunel, A.O. 2019. Accuracy assesment of a low-cost UAV derived digital elevation model (DEM) in a highly broken and vegetated terrain. Measurement: Journal of the International Measurement Confederation 136:382–386. https://doi.org/10.1016/j.measurement.2018.12.101

Alderete, M.S. 2020. Análise do risco toxicológico e sua implicação no planejamento territorial: estudo de caso do arsênio e do cádmio no Alto do Rio das Velhas. Universidade Federal de Ouro Preto.

Aleotti, P. E Chowdhury, R. 1999. Landslide hazard assessment: summary review and new perspectives. Bulletin of Engineering Geology and the Environment, 58:21-44.

Alkmim F.F. & Martins-Neto M.A. 2012. Proterozoic first-order sedimentary sequences of the São Francisco craton, eastern Brazil. Marine and Petroleum Geology, 33:127-139.

Alkmim, F. F., & Marshak, S. 1998. Transamazonian orogeny in the Southern Sao Francisco craton region, Minas Gerais, Brazil: evidence for Paleoproterozoic collision and collapse in the Quadrilátero Ferrıfero. Precambrian Research, 90:29-58.

Almeida L. G. 2004. Evolução Tectônica da porção central do sinclinal Dom Bosco, Quadrilátero Ferrífero - Minas Gerais. Dep. de Geologia da Universidade Federal de Ouro Preto. Dissertação de mestrado, 110p.

Almeida, F.F.M. 1977. O Cráton do São Francisco. Revista Bras. Geociências, 7: 349–364.

Amato, G., Eisank, C., Castro-Camilo, D., Lombardo, L. 2019. Accounting for covariate distributions in slope-unit-based landslide susceptibility models. A case study in the alpine environment. Engineering Geology 260. https://doi.org/10.1016/j.enggeo.2019.105237

Atkinson, P.M., Massari, R. 1998. Generalised linear modelling of susceptibility to landsliding in the central Apennines, Italy. Computers and Geosciences 24:373–385. https://doi.org/10.1016/S0098-3004(97)00117-9

Ba, Q., Chen, Y., Deng, S., Wu, Q., Yang, J., Zhang, J. 2017. An improved information value model based on gray clustering for landslide susceptibility mapping. ISPRS International Journal of Geo-Information 6. https://doi.org/10.3390/ijgi6010018

Bălteanu, D., Chendeş, V., Sima, M., Enciu, P. 2010. A country-wide spatial assessment of landslide susceptibility in Romania. Geomorphology 124:102–112. https://doi.org/10.1016/j.geomorph.2010.03.005

Banerjee, P., Ghose, M.K., Pradhan, R. 2018. Analytic hierarchy process and information value method-based landslide susceptibility mapping and vehicle vulnerability assessment along a highway in Sikkim Himalaya. Arabian Journal of Geosciences 11. https://doi.org/10.1007/s12517-018-3488-4

Barella, C.F. 2016. Abordagens Estatísticas Aplicadas Ao Mapeamento De Susceptibilidade a Movimentos De Massa: Análise De Diferentes Técnicas No Contexto Do Quadrilátero Ferrífero. Universidade Federal de Ouro Preto.

Barella, C.F., Sobreira, F.G., Zêzere, J.L. 2019. A comparative analysis of statistical landslide susceptibility mapping in the southeast region of Minas Gerais state, Brazil. Bulletin of Engineering Geology and the Environment 78:3205–3221. https://doi.org/10.1007/s10064-018-1341-3

Barbosa, J.S.F., Barbosa, R.G. 2017. The Paleoproterozoic Eastern Bahia Orogenic Domain. In: U.G. Cordani et al. (eds.), São Francisco Craton, Eastern Brazil, Regional Geology Reviews, 57-69.

Barredo, J.I., Benavides, A., Hervas, J.E van Westen, C.J. 2000. Comparing heuristic landslide hazard assessment techniques using GIS in the Tirajana basin, Gran Canaria Island, Spain. International Journal of Applied Earth Observation and Geoinformation 2:9–23.

Baum, R. L., Savage, W. Z., & Godt, J. W. 2002. TRIGRS—A Fortran Program for Transient Rainfall Infiltration and Grid-Based Regional Slope-Stability Analysis. USGS Open-file Report number 02-424:1-61.

Blahut, J., van Westen, C.J., Sterlacchini, S. 2010. Analysis of landslide inventories for accurate prediction of debris-flow source areas. Geomorphology 119:36–51. https://doi.org/10.1016/j.geomorph.2010.02.017

Camilo, D.C., Lombardo, L., Mai, P.M., Dou, J., Huser, R. 2017. Handling high predictor dimensionality in slope-unit-based landslide susceptibility models through LASSO-penalized Generalized Linear Model. Environmental Modelling and Software 97:145–156. https://doi.org/10.1016/j.envsoft.2017.08.003

Carrara, A. 1993. Uncertainty in Evaluating Landslide Hazard and Risk. National Research Council-CIOC 101–109. https://doi.org/10.1007/978-94-015-8190-5_12

Carneiro M. A. 1992. O Complexo Metamórfico Bonfim Setentrional - Quadrilátero Ferrífero, Minas Gerais: Litoestratigrafia e evolução geológica de um segmento de crosta continental do Arqueano. Tese de Doutoramento, Instituto de Geociências, Universidade de São Paulo, 233p.

Carneiro, M.A., Noce, C.M., Teixeira, W. 1995. Evolução tectônica do Quadrilátero Ferrífero sob o ponto de vista da Geocronologia. Revista da Escola de Minas, 48: 264–274.

Castro, J.M.G. 2006. Pluviosidade e movimentos de massa nas encostas de Ouro Preto. Universidade Federal de Ouro Preto.

Chen, T., Niu, R., Jia, X. 2016. A comparison of information value and logistic regression models in landslide susceptibility mapping by using GIS. Environmental Earth Sciences 75. https://doi.org/10.1007/s12665-016-5317-y

Chen, W., Li, W., Chai, H., Hou, E., Li, X., Ding, X. 2016. GIS-based landslide susceptibility mapping using analytical hierarchy process (AHP) and certainty factor (CF) models for the Baozhong region of Baoji City, China. Environmental Earth Sciences 75:1–14. https://doi.org/10.1007/s12665-015-4795-7

Chen, W., Li, Y. 2020. GIS-based evaluation of landslide susceptibility using hybrid computational intelligence models. Catena 195. https://doi.org/10.1016/j.catena.2020.104777

Chung, C.J.F., Fabbri, A.G. 1999. Probabilistic prediction models for landslide hazard mapping. Photogrammetric Engineering and Remote Sensing 65:1389–1399.

Chung, C.-J.F., Fabbri, A.G. 2003. Validation of Spatial Prediction Models for Landslide Hazard Mapping. Natural Hazards 30:451–472. https://doi.org/10.1023/B:NHAZ.0000007172.62651.2b

Constantin, M., Bednarik, M., Jurchescu, M.C., Vlaicu, M. 2011. Landslide susceptibility assessment using the bivariate statistical analysis and the index of entropy in the Sibiciu Basin (Romania). Environmental Earth Sciences 63:397–406. https://doi.org/10.1007/s12665-010-0724-y

Corominas, J., van Westen, C., Frattini, P., Cascini, L., Malet, J.P., Fotopoulou, S., Catani, F., Van Den Eeckhaut, M., Mavrouli, O., Agliardi, F., Pitilakis, K., Winter, M.G., Pastor, M., Ferlisi, S., Tofani, V., Hervás, J., Smith, J.T. 2014. Recommendations for the quantitative analysis of landslide risk. Bulletin of Engineering Geology and the Environment 73:209–263. https://doi.org/10.1007/s10064-013-0538-8

Corominas, J.D., Mavrouli, O.C. 2011. Rockfall quantitative risk assessment, in: Rockfall Engineering. ISTE/WILEY, 255–301.

Corteletti, R.C. 2017. Metodologia para análise de riscos geológico-geotécnicos em ferrovias: Estrada de Ferro Carajás (EFC), Editora UFOP.

CPRM 2016. Ação Emergencial para reconhecimento de áreas de alto e muito alto risco a movimentos de massa e enchentes. Relatório de atualização de mapeamento, Ouro Preto-MG. 60.

de Paula, S.F., Castro, P. de T.A. 2015. Geomorfologia antropogênica em função da mineração de ouro no século XVIII: bases científicas e educativas na proposição de uma Trilha Geoturística Urbana na Sede no Município de Ouro Preto (MG). Revista Brasileira de Ecoturismo (RBEcotur) 8:432–443. https://doi.org/10.34024/rbecotur.2015.v8.6465

Dorr, J. 1969. Physiographic, Stratigraphic and Structural Development of the Quadrilatero Ferrifero, Minas Gerais, Brazil. US Geological Survey Professional Paper.

Dorr J. V. N. II., Gair J. E., Pomerene J. B., Rynearson G. A. 1957. Revisão Estratigráfica Pré-Cambriana do Quadrilátero Ferrífero. Rio de Janeiro, DNPM/DFPM. Avulso. 81. 36p.

Du, G. liang, Zhang, Y. shuang, Iqbal, J., Yang, Z. hua, Yao, X. 2017. Landslide susceptibility mapping using an integrated model of information value method and logistic regression in the Bailongjiang watershed, Gansu Province, China. Journal of Mountain Science 14:249–268. https://doi.org/10.1007/s11629-016-4126-9

Ferreira, S.D.E.P. 2018. Proposta Metodologica de Avaliação do Índice de Vulnerabilidade Física de Moradias em Áreas de Escorregamentos e o Valor Monetário de Perda Associado - Estudo de Caso: Distrito Sede de Ouro Preto.

Fell, R. 1994. Landslide risk assessment and acceptable risk. Canadian Geotechinical Jornal. 31:261-272.

Fell, R.; Corominas, J.; Bonnard, C.; Cascini, L.; Leroi, E.; Savage, W.Z. 2008. Guidelines for landslide susceptibility, hazard and risk zoning for land use planning. Engineering Geology, 85-98.

Fernandes N.F., Guimarães R.F., Gomes R.A.T., Vieira B.C., Montgomery D.R. E Greenberg H. 2001. Condicionantes geomorfológicos dos deslizamentos nas encostas: avaliação de metodologias e aplicação de modelo de previsão de áreas susceptíveis. Revista Brasileira de Geomorfologia, 2:51-71.

Fernandes, N. F. & Amaral, C. P. 1996. Movimentos de massa: uma abordagem geológico-geomorfológica. Geomorfologia e Meio Ambiente. Bertrand, Rio de Janeiro. p. 123-194.

Fontes, M.M.M. 2011. Contribuição para o desenvolvimento da metodologia de análise, gestão e controle de riscos geotécnicos para a área urbana da cidade de Ouro Preto. Revista Trabalho Necessário. Universidade Federal de Ouro Preto. https://doi.org/10.22409/tn.17i34.p38061

Fontes, S.B. 1999. Mapeamento geotécnico com ênfase em erosões no município de Ouro Preto - MG. Escala 1:5000. Universidade de São Paulo.

Garcia, R.A.C. 2012. Metodologias de avaliação da perigosidade e risco associado a movimentos de vertente: Aplicação na bacia do rio Alenquer. Universidade de Lisboa.

Goetz, J.N., Brenning, A., Petschko, H., Leopold, P. 2015. Evaluating machine learning and statistical prediction techniques for landslide susceptibility modeling. Computers and Geosciences 81:1–11. https://doi.org/10.1016/j.cageo.2015.04.007

Guri, P.K., Champati ray, P.K., Patel, R.C. 2015. Spatial prediction of landslide susceptibility in parts of Garhwal Himalaya, India, using the weight of evidence modelling. Environmental Monitoring and Assessment 187. https://doi.org/10.1007/s10661-015-4535-1

Guthrie, R.H., Evans, S.G. 2004. Analysis of landslide frequencies and characteristics in a natural system, coastal British Columbia. Earth Surface Processes and Landforms 29:1321–1339. https://doi.org/10.1002/esp.1095

Gomes, R.A.T., Guimarães, R.F., Carvalho JR, O.A. & Fernandes, N.F. 2005. Análise de um modelo de previsão de deslizamentos (SHALSTAB) em diferentes escalas cartográficas. Solos e Rochas, 28:85-97.

Guzzetti, F., Carrara, A., Cardinali, M. E Reichenbach, P. 1999. Landslide hazard evaluation: a review of current techniques and their application in a multi-scale study, Central Italy. Geomorphology, 31:181–216.

Guzzetti, F., Manunta, M., Ardizzone, F., Pepe, A., Cardinali, M., Zeni, G., Reichenbach, P., Lanari, R. 2009. Analysis of ground deformation detected using the SBAS-DInSAR technique in Umbria, Central Italy. Pure and Applied Geophysics 166:1425–1459. https://doi.org/10.1007/s00024-009-0491-4

Guzzetti, F., Reichenbach, P., Ardizzone, F., Cardinali, M., Galli, M. 2006. Estimating the quality of landslide susceptibility models. Geomorphology 81:166–184. https://doi.org/10.1016/j.geomorph.2006.04.007

Hasui, Y., Carneiro, C.D.R., Almeida, F.F.M., Bartorelli, A..2012. Geologia do Brasil. São Paulo. Beca

Herz, N. 1970. Gneissic and igneous rocks of the Quadrilátero Ferrífero, Minas Gerais, Brazil. U.S. Geological Survey Professional Paper, 641-B:1-58.

Hurley,P.M., Almeida, F.F.M.,Melcher,G.C., Cordani, U.G., Rand, J.R., Kawashita, K., Vandoros, P., Pinson, W.H., Fairbairn, H.W. 1967. Test of continental drift by comparioson of radiometric ages. Science, 157: 495–500.

Heckmann, T., Gegg, K., Gegg, A., Becht, M. 2014. Sample size matters: Investigating the effect of sample size on a logistic regression susceptibility model for debris flows. Natural Hazards and Earth System Sciences 14:259–278. https://doi.org/10.5194/nhess-14-259-2014

Huang, Y., Zhao, L. 2018. Review on landslide susceptibility mapping using support vector machines. Catena 165:520–529. https://doi.org/10.1016/j.catena.2018.03.003

ISSMGE TC32. 2004. Technical Committee on Risk Assessment and Management Glossary of Risk Assessment Terms.

Imaizumi, F., Sidle, R.C. 2007. Linkage of sediment supply and transport processes in Miyagawa Dam catchment, Japan. Journal of Geophysical Research: Earth Surface 112:1–17. https://doi.org/10.1029/2006JF000495

Imaizumi, F., Sidle, R.C., Kamei, R. 2007. Effects of forest harvesting on the occurrence of landslides and debris flows in steep terrain of central Japan. Earth Surface Processes and Landforms 33:827–840. https://doi.org/10.0.3.234/esp.1574

Innes, J.L. 1983. Lichenometric dating of debris-flow deposits in the Scottish Highlands. Earth Surface Processes and Landforms 8:579–588. https://doi.org/10.1002/esp.3290080609

Julião, R.P., Nery, F., Ribeiro, J.L., Branco, M.C. E Zêzere, J.L. 2009. Guia Metodológico para a Produção de Cartografia Municipal de Risco e para a Criação de Sistemas de Informação Geográfica (SIG) de Base Municipal. Autoridade Nacional de Protecção Civil – ANPC. Portugal. 91p.

Kadavi, P.R., Lee, C.W., Lee, S. 2018. Application of ensemble-based machine learning models to landslide susceptibility mapping. Remote Sensing 10:1–18. https://doi.org/10.3390/rs10081252

Kohavi, R. 1996. Scaling Up the Accuracy of Naive-Bayes Classifiers: a Decision-Tree Hybrid. Data Mining and Visualization 1–6.

Korup, O. 2005. Distribution of landslides in southwest New Zealand. Landslides 2:43–51. https://doi.org/10.1007/s10346-004-0042-0

Li, C., Fu, Z., Wang, Y., Tang, H., Yan, J., Gong, W., Yao, W., Criss, R.E. 2019. Susceptibility of reservoir-induced landslides and strategies for increasing the slope stability in the Three Gorges Reservoir Area: Zigui Basin as an example. Engineering Geology 261. https://doi.org/10.1016/j.enggeo.2019.105279

Lobato, L.M., Achstschin, A.B., Baars, F.J., Baltazar, O.F., Timbó, M.A., Reis, L.B., Voll, E., Silva, S.L. da, Berni, G.V., Silveira, V.D., Versiani, B.R., Ferreira, M. e D.V. 2005. Projeto Geologia do Quadrilátero Ferrífero - Integração e Correção Cartográfica em SIG com Nota Explicativa. Belo Horizonte.

Machado N. & Carneiro M.A. 1992. U-Pb evidence of late Archean tectono-thermal activity in the southern São Francisco shield, Brazil. Can. J. Earth Sci. 29:2341-2346.

Machado N. & Noce C.M. 1993. A evolução do Setor Sul do Cráton São Francisco entre 3,1 e 0,5 Ga baseada em geocronologia U-Pb. In: SIMP. CRATON SÃO FRANCISCO, 2. Salvador, 1993. Anais...Salvador, SBG-BA, SE/SBG. p.100-102.

Machado N., Noce C. M., Oliveira O. A. B. de, Ladeira, E. A. 1989. Evolução geológica do Quadrilátero Ferrífero no Arqueano e Proterozóico Inferior, com base em geocronologia U-Pb. In: SIMPÓSIO GEOLOGIA MINAS GERAIS 5 E SIMPÓSIO GEOLOGIA BRASILIA 1, Belo Horizonte, 1989. Anais Belo Horizonte, SBG/NMG. p.1-5.

Machado N., Noce C.M., Ladeira E.A., Belo de Oliveira, O.A. 1992. U-Pb geochronology of Archean magmatism and Proterozoic metamorphism in the Quadrilátero Ferrífero, southern São Francisco Craton, Brazil. Geol. Soc. Amer. Bull., 104:1221-1227.

Machado, N., Schrank, A., Noce, C.M., Gauthier, G. 1996. Ages of detrital zircon from ArcheanPaleoproterozoic sequences Implications for Greenstone Belt setting and evolution of a Transamazonian foreland basin in Quadrilátero Ferrífero, southeast Brazil. Earth and Planetary Science Letters 141: 259-276.

Maxwell C. H. 1958. The Batatal Formation. Sociedade Brasileira de Geologia, Bol. vol. 7 n°2, p. 60-61

Montgomery, D.R. & Dietrich, W.E. 1994. A physically based model for the topographic control on shallow landsliding. Water Resources Research, 30:1153- 1171.

Pack, R.T., Tarboton, D.G. & Goodwin, C.N. 1998. The SINMAP approach to terrain stability mapping. 8th Congress of the International Association of Engineering Geology, IAEG, Vancouver, Canada, 3: 1157-1165.

Nhu, V.H., Hoang, N.D., Nguyen, H., Ngo, P.T.T., Thanh Bui, T., Hoa, P.V., Samui, P., Tien Bui, D. 2020. Effectiveness assessment of Keras based deep learning with different robust optimization algorithms for shallow landslide susceptibility mapping at tropical area. Catena 188. https://doi.org/10.1016/j.catena.2020.104458

Nohani, E., Moharrami, M., Sharafi, S., Khosravi, K., Pradhan, B., Pham, B.T., Lee, S., Melesse, A.. 2019. Landslide Susceptibility Mapping Using Different GIS-Based Bivariate Models. Water 11.

Oliveira, S.C. 2010. Incidência Espacial e Temporal da Instabilidade Geomorfológica na Bacia do Rio Grande da Pipa (Arruda dos Vinhos). Universidade de Lisboa.

Oliveira, S. C., Rocha, J., Zêzere, J. L., Garcia, R. A. C. & Piedade, A. 2009. Avaliação da susceptibilidade a deslizamentos rotacionais através da aplicação de métodos estatísticos, in: Lidel (Ed.), VI Conferência Nacional de Cartografia E Geodesia – Conhecer O Território, Sustentar O Desenvolvimento. Ordem dos Engenheiros, Caldas da Rainha 530–539.

Oliveira, S.C., Zêzere, J.L., Catalão, J., Nico, G. 2015. The contribution of PSInSAR interferometry to landslide hazard in weak rock-dominated areas. Landslides 12:703–719. https://doi.org/10.1007/s10346-014-0522-9

Pardeshi, S.D., Autade, S.E., Pardeshi, S.S. 2013. Landslide hazard assessment: recent trends and techniques. SpringerPlus 2, 523. https://doi.org/10.1186/2193-1801-2-523

Pereira, S., Zêzere, J.L., Bateira, C. 2012. Technical Note: Assessing predictive capacity and conditional independence of landslide predisposing factors for shallow landslide susceptibility models. Natural Hazards and Earth System Science 12:979–988. https://doi.org/10.5194/nhess-12-979-2012

Pereira, S., Garcia, R.A.C., Zêzere, J.L., Oliveira, S.C., Silva, M. 2017. Landslide quantitative risk analysis of buildings at the municipal scale based on a rainfall triggering scenario. Geomatics, Natural Hazards and Risk 8:624–648. https://doi.org/10.1080/19475705.2016.1250116

Pereira, S.S. 2009. Perigosidade a Movimentos de Vertente na Região Norte de Portugal. Tese de Doutorado, Faculdade de Letras da Universidade do Porto, Universidade do Porto. Porto, Portugal, 370p.

Piedade A.M.M. 2009. Modelação Espacial em Sistemas de Informações Geográficas da Suscetibilidade a deslizamentos na Área de Lousa-Loures. Dissertação de Mestrado, Faculdade de Ciências Sociais e Humanas, Universidade Nova de Lisboa. Lisboa, Portugal. 114p.

Pomerene J. B. 1958a. The Cercadinho Formation.: Sociedade Brasileira de Geologia, Bol. vol.7, n°2, p.64-65.

Pomerene J. B. 1958b. The Barreiro Formation: Sociedade Brasileira de Geologia, Bol. vol. 7, nº2, p. 67-68.

Petschko, H., Brenning, A., Bell, R., Goetz, J., Glade, T. 2014. Assessing the quality of landslide susceptibility maps - Case study Lower Austria. Natural Hazards and Earth System Sciences 14:95–118. https://doi.org/10.5194/nhess-14-95-2014

Petschko, H., Bell, R., Leopold, P., Heiss, G., Glade, T. 2013. Landslide Science and Practice. Landslide Science and Practice 1:281–286. https://doi.org/10.1007/978-3-642-31325-7

Pham, B.T., Nguyen-Thoi, T., Qi, C., Phong, T. Van, Dou, J., Ho, L.S., Le, H. Van, Prakash, I. 2020. Coupling RBF neural network with ensemble learning techniques for landslide susceptibility mapping. Catena 195. https://doi.org/10.1016/j.catena.2020.104805

Pham, B.T., Prakash, I. 2019. A novel hybrid model of Bagging-based Naïve Bayes Trees for landslide susceptibility assessment. Bulletin of Engineering Geology and the Environment 78:1911–1925. https://doi.org/10.1007/s10064-017-1202-5

Pham, B.T., Prakash, I., Tien Bui, D. 2018. Spatial prediction of landslides using a hybrid machine learning approach based on Random Subspace and Classification and Regression Trees. Geomorphology 303:256–270. https://doi.org/10.1016/j.geomorph.2017.12.008

Ponçano, W.L., Carneiro, C.D.R., Almeida, M.A., Pires Neto, A.G., Almeida, F.F.M. 1979. O conceito de sistemas de relevo aplicado ao mapeamento geomorfológico do estado de São Paulo, in: 2° Simpósio Regional de Geologia. SBG, Rio Claro, 253–262.

Pourghasemi, H.R., Gayen, A., Park, S., Lee, C.W., Lee, S. 2018. Assessment of landslide-prone areas and their zonation using logistic regression, LogitBoost, and naïvebayes machine-learning algorithms. Sustainability (Switzerland) 10. https://doi.org/10.3390/su10103697

Reichenbach, P., Rossi, M., Malamud, B.D., Mihir, M., Guzzetti, F. 2018. A review of statistically-based landslide susceptibility models. Earth-Science Reviews 180:60–91. https://doi.org/10.1016/j.earscirev.2018.03.001

Reis, L.A., Martins-Neto, M.A., Gomes, N.S., Endo, I. 2002. A bacia de antepaís paleoproterzóica Sabará, Quadrilátero Ferrífero, MG. Revista Brasileira de Geociências, 32:43- 58.

Rice, R.M., Crobett, E.S., Bailey, R.G. 1969. Soil Slips Related to Vegetation, Topography, and Soil in Southern California. Water Resources Research 5:647–659. https://doi.org/10.1029/WR005i003p00647

Rossi, D.Q. 2014. Estratigrafia e arcabouço estrutural da regioão de Fábrica Nova, Quadrilátero Ferrífero, Minas Gerais. Mestrado. Universidade Federal de Ouro Preto.

Rosa, M.L. 2018. Cartografia de suscetibilidade a deslizamentos utilizando o método estatístico “Valor Informativo”: Estudo de caso na bacia do Ribeirão dos Macacos, Nova Lima/MG. Dissertação de Mestrado, Programa de Pós-graduação em Evolução Crustal e Recursos Naturais da UFOP, Universidade Federal de Ouro Preto, 72p.

Schlögel, R., Marchesini, I., Alvioli, M., Reichenbach, P., Rossi, M., Malet, J.P. 2018. Optimizing landslide susceptibility zonation: Effects of DEM spatial resolution and slope unit delineation on logistic regression models. Geomorphology 301:10–20. https://doi.org/10.1016/j.geomorph.2017.10.018

Shahabi, H., Hashim, M. 2015. Landslide susceptibility mapping using GIS-based statistical models and Remote sensing data in tropical environment. Scientific Reports 5.

Sharma, S., Mahajan, A.K. 2018. A comparative assessment of information value , frequency ratio and analytical hierarchy process models for landslide susceptibility mapping of a Himalayan watershed , India. Bulletin of Engineering Geology and the Environment 2431–2448.

Shirzadi, A., Bui, D.T., Pham, B.T., Solaimani, K., Chapi, K., Kavian, A., Shahabi, H., Revhaug, I. 2017. Shallow landslide susceptibility assessment using a novel hybrid intelligence approach. Environmental Earth Sciences 76. https://doi.org/10.1007/s12665-016-6374-y

Simmons G.C. 1968. Geology and ore deposits of the Western serra do Curral, Minas Gerais, Brazil. USGS Prof. Paper, 341- G, 57 p.

Sobreira, F. G. 2014. Mineração do ouro no período colonial: alterações paisagísticas antrópicas na serra de Ouro Preto, Minas Gerais. Quaternary and Environmental Geosciences, 5:55-65.

Sobreira, F.G. E Souza, L.A. 2012. Cartografia geotécnica aplicada ao planejamento urbano. Revista Brasileira de Geologia de Engenharia e Ambiental, 2:79-97.

Sobreira, F. G.; Fonseca, M. A. 2001. Impactos físicos e sociais de antigas actividades de mineração em Ouro Preto, Brasil. Geotecnia (Lisboa), Lisboa Portugal, 92:5-28.

Sobreira, F.G.; Araújo, L.G. 1992. Proposta de metodologia para o enfrentamento do problema das encostas em Ouro Preto. REM – Revista Escola de Minas, 45:208-209.

Soeters, R. E van Westen, C.J. 1996. Slope instability recognition, analysis, and zonation. Landslides: Investigation and Mitigation, A.K. Turner e R.L. Shuster (eds.), Transportation Research Board, National Research Council, special Report 247:129-177.

Süzen, M.L. & Doyuran, V. 2004. A comparison of the GIS based landslide susceptibility assessment methods: multivariate versus bivariate. Environmental Geology, 45(5): 665-679.

Sun, X., Chen, J., Han, X., Bao, Y., Zhan, J., Peng, W. 2020. Application of a GIS-based slope unit method for landslide susceptibility mapping along the rapidly uplifting section of the upper Jinsha River, South-Western China. Bulletin of Engineering Geology and the Environment 79:533–549. https://doi.org/10.1007/s10064-019-01572-5

Süzen, M.L., Doyuran, V. 2004. Data driven bivariate landslide susceptibility assessment using geographical information systems: A method and application to Asarsuyu catchment, Turkey. Engineering Geology 71, 303–321. https://doi.org/10.1016/S0013-7952(03)00143-1

Thiery, Y., Malet, J.P., Sterlacchini, S., Puissant, A., Maquaire, O. 2007. Landslide susceptibility assessment by bivariate methods at large scales: Application to a complex mountainous environment. Geomorphology 92:38–59. https://doi.org/10.1016/j.geomorph.2007.02.020

Tominaga, L.K. 2007. Avaliação de Metodologias de Análise de Risco a Escorregamentos: Aplicação de um Ensaio em Ubatuba, SP. Dissertação de Mestrado, Faculdade de Filosofia, Letras e Ciências Humanas, USP, São Paulo, SP, 220p.

USGS. 2008. The landslide handbook – A guide to understanding landslides. Highland, L.M., and Bobrowsky, P.: Reston, Virginia, U.S. Geological Survey Circular. GFDRR/World Bank. 1325, 129p.

van Den Eeckhaut, M., Vanwalleghem, T., Poesen, J., Govers, G., Verstraeten, G., Vandekerckhove, L. 2006. Prediction of landslide susceptibility using rare events logistic regression: A case-study in the Flemish Ardennes (Belgium). Geomorphology 76:392–410. https://doi.org/10.1016/j.geomorph.2005.12.003

van Westen, C.J. 2000. The modelling of landslide hazards using gis. Surveys in Geophysics, 21:241-255.

van Westen, C.J., Rengers, N. & Soeters, R. 2003. Use of geomorphological information in indirect landslide susceptibility assessment. Natural Hazards, 30(3): 399-419.

Varnes, D.J. 1984. Landslide hazard zonation: A review of principles and practice. IAEG Monograph 59.

Varnes, D.J. 1978. Slope Movement Types and Processes, in: Landslides: Analysis and Control. Transportation Research Board, Washington, DC, 11–33.

Wang, F., Xu, P., Wang, C., Wang, N., Jiang, N. 2017. Application of a gis-based slope unit method for landslide susceptibility mapping along the longzi river, southeastern tibetan plateau, China. ISPRS International Journal of Geo-Information 6. https://doi.org/10.3390/ijgi6060172

Xavier, M.O. 2018. Mapeamento da susceptibilidade a movimentos gravitacionais de massa utilizando a análise estatística do valor informativo aplicada ao distrito sede da cidade histórica de Ouro Preto-MG. Universidade Federal de Ouro Preto.

Xiao, T., Segoni, S., Chen, L., Yin, K., Casagli, N. 2020. A step beyond landslide susceptibility maps: a simple method to investigate and explain the different outcomes obtained by different approaches. Landslides 17:627–640. https://doi.org/10.1007/s10346-019-01299-0

Zêzere, J.L. 2002. Landslide susceptibility assessment considering landslide typology. A case study in the area north of Lisbon (Portugal). Natural Hazards and Earth System Sciences 2:73–82. https://doi.org/10.5194/nhess-2-73-2002

Zêzere, J.L., Pereira, S., Melo, R., Oliveira, S.C., Garcia, R.A.C. 2017. Mapping landslide susceptibility using data-driven methods. Science of the Total Environment 589:250–267. https://doi.org/10.1016/j.scitotenv.2017.02.188

Zêzere, J., Henriques, C., Garcia, R., Oliveira, S., Piedade, A., Neves, M. 2009. Effects of landslide inventories uncertainty on landslide susceptibility modelling, in: Procedings of the Landslide Processes. From Geomorphologic Mapping to Dynamic Modeling Conference. A Tribute to Prof. Theo van Asch. 81–86.

Zêzere, J.L., Garcia, R.A.C., Oliveira, S.C. & Reis, E. 2005. Análise sensitiva na avaliação da susceptibilidade a deslizamentos na região a norte de Lisboa. X Colóquio Ibérico de Geografia, APG, Évora, PT.

Zucchetti, M., Lobato, L.M., Baltazar, O.F. 2000. Volcanic and volcaniclastic featuresin Archean rocks and their tectonic environment, Rio das Velhas Greenstone Belt, Quadrilátero Ferrífero, MG. Brazil. Revista Brasileira de Geociências, 30: 388-39

Zuquette, L.V. 1993. Importância do mapeamento geotécnico no uso e ocupação do meio físico: fundamento e guia para elaboração. 2v. Tese. Escola de Engenharia da Universidade de São Paulo, São Carlos. 368p.

Zhu, A.X., Miao, Y., Yang, L., Bai, S., Liu, J., Hong, H. 2018. Comparison of the presence-only method and presence-absence method in landslide susceptibility mapping. Catena 171:222–233. https://doi.org/10.1016/j.catena.2018.07.012

Zizioli, D., Meisina, C., Valentino, R., Montrasio, L. 2013. Comparison between different approaches to modeling shallow landslide susceptibility: A case history in Oltrepo Pavese, Northern Italy. Natural Hazards and Earth System Sciences 13:559–573. https://doi.org/10.5194/nhess-13-559-2013

APPENDIX

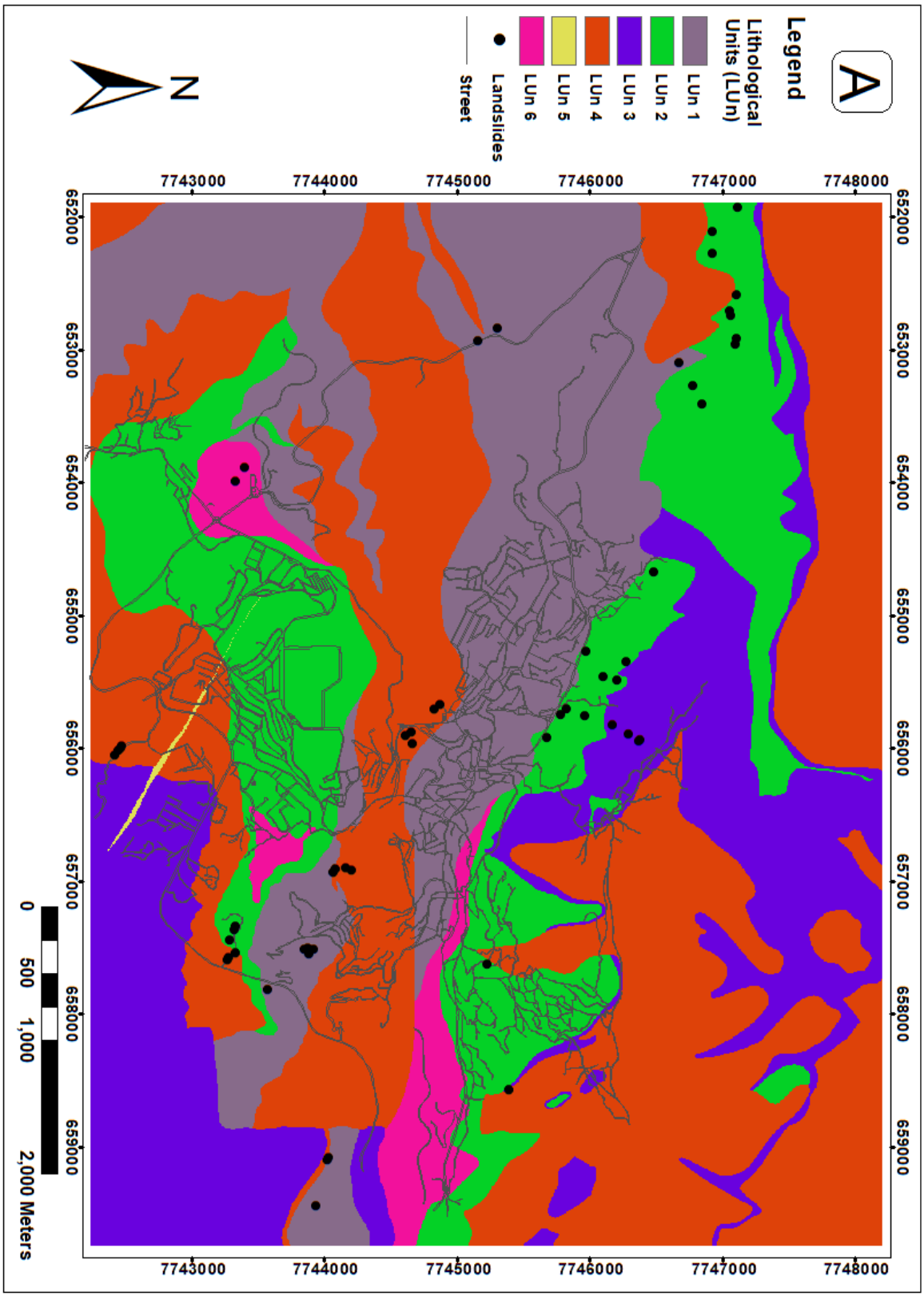
A
Legend
Lithological Units (LUn)
LUn 1
LUn 2
LUn 3
LUn 4
LUn 5
LUn 6
Landslides
Street
N
7743000
7744000
7745000
7746000
7747000
7748000
652000
653000
654000
655000
656000
657000
658000
659000
0
500
1,000
2,000 Meters

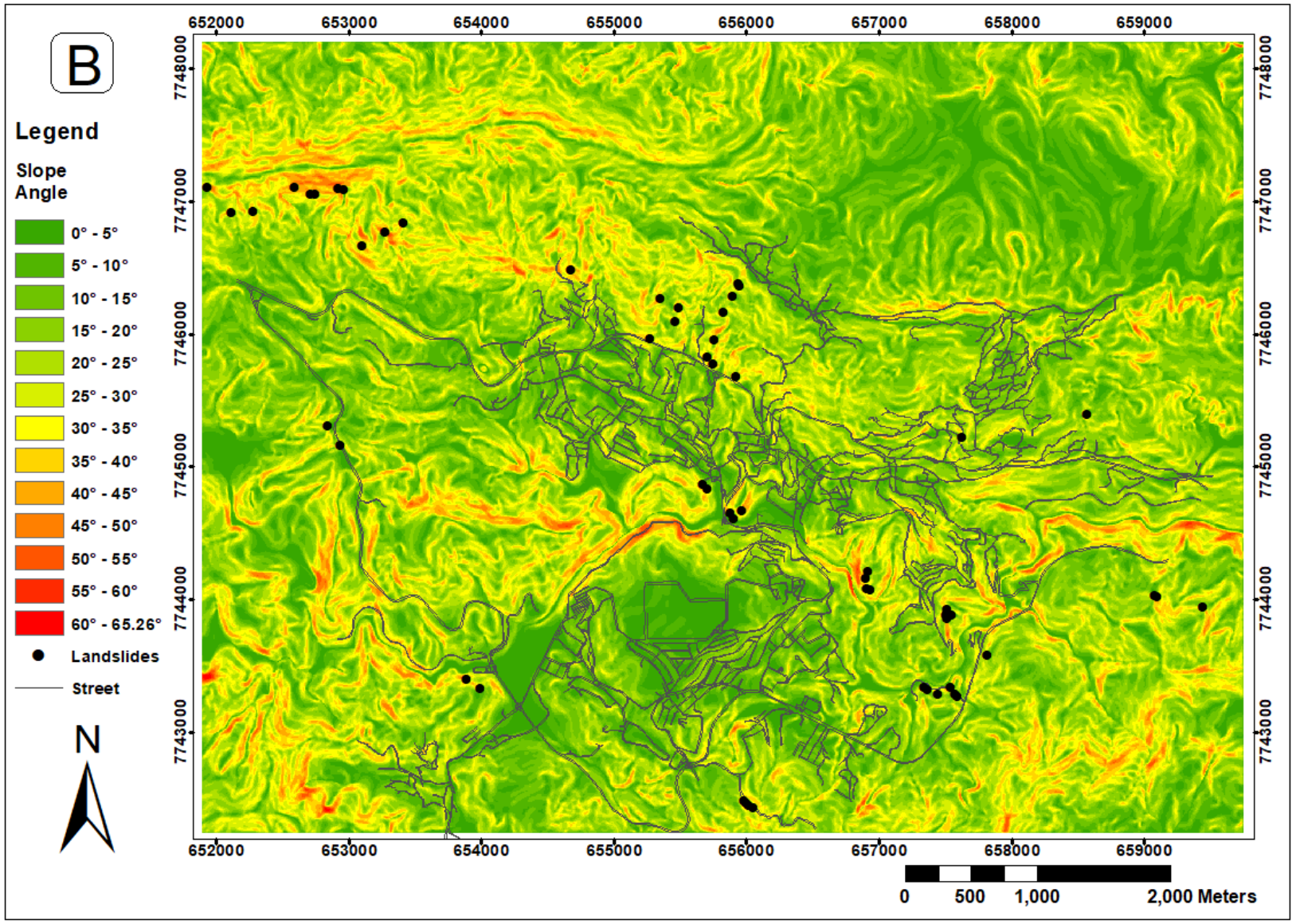
B
Legend
Slope Angle
0° - 5°
5° - 10°
10° - 15°
15° - 20°
20° - 25°
25° - 30°
30° - 35°
35° - 40°
40° - 45°
45° - 50°
50° - 55°
55° - 60°
60° - 65.26°
Landslides
Street
N
652000
653000
654000
655000
656000
657000
658000
659000
7748000
7747000
7746000
7745000
7744000
7743000
0
500
1,000
2,000 Meters

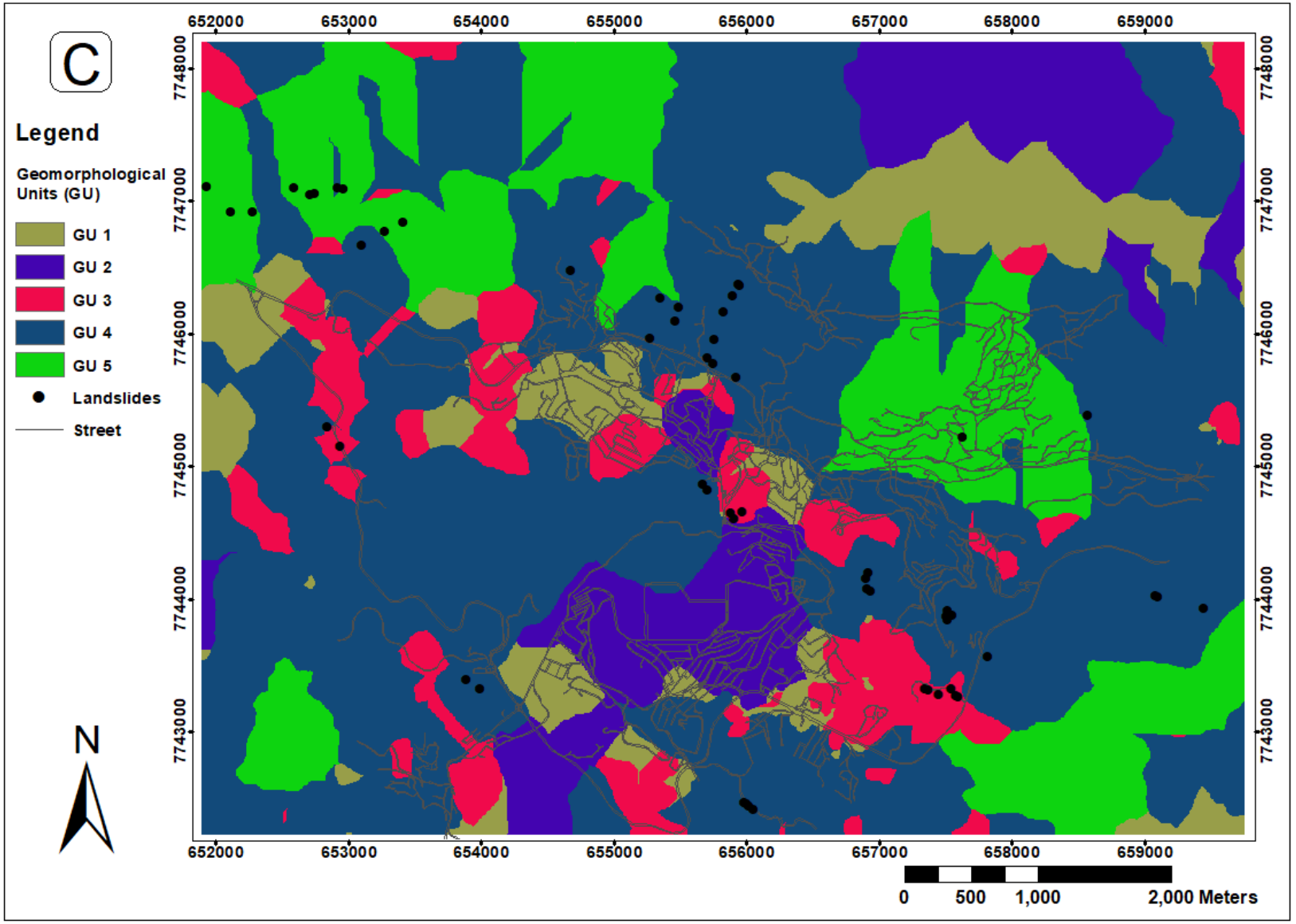
C
Legend
Geomorphological Units (GU)
GU 1
GU 2
GU 3
GU 4
GU 5
Landslides
Street
N
652000
653000
654000
655000
656000
657000
658000
659000
7748000
7747000
7746000
7745000
7744000
7743000
0
500
1,000
2,000 Meters

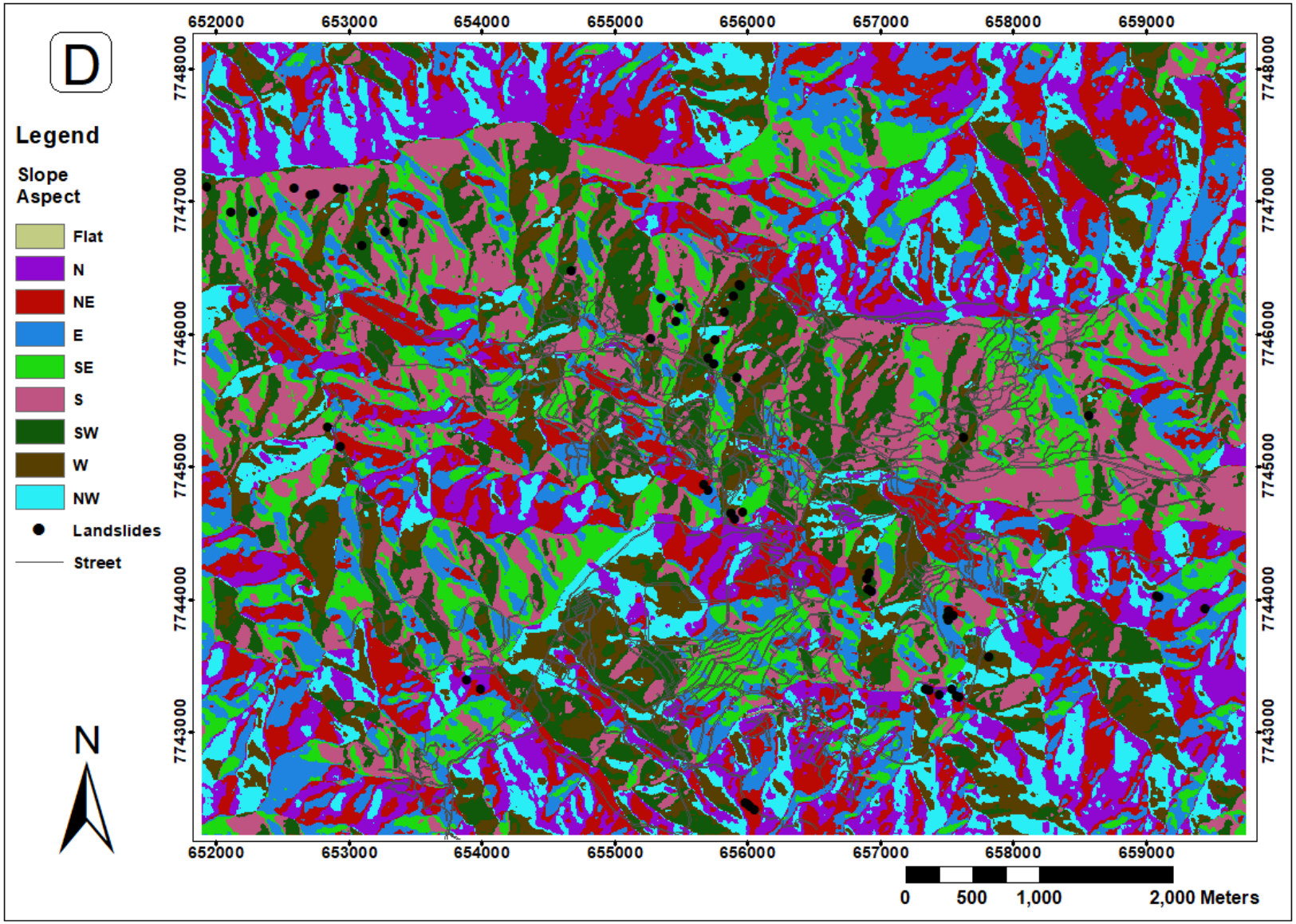
D
Legend
Slope Aspect
Flat
N
NE
E
SE
S
SW
W
NW
Landslides
Street
652000
653000
654000
655000
656000
657000
658000
659000
7748000
7747000
7746000
7745000
7744000
7743000
N
0
500
1,000
2,000 Meters

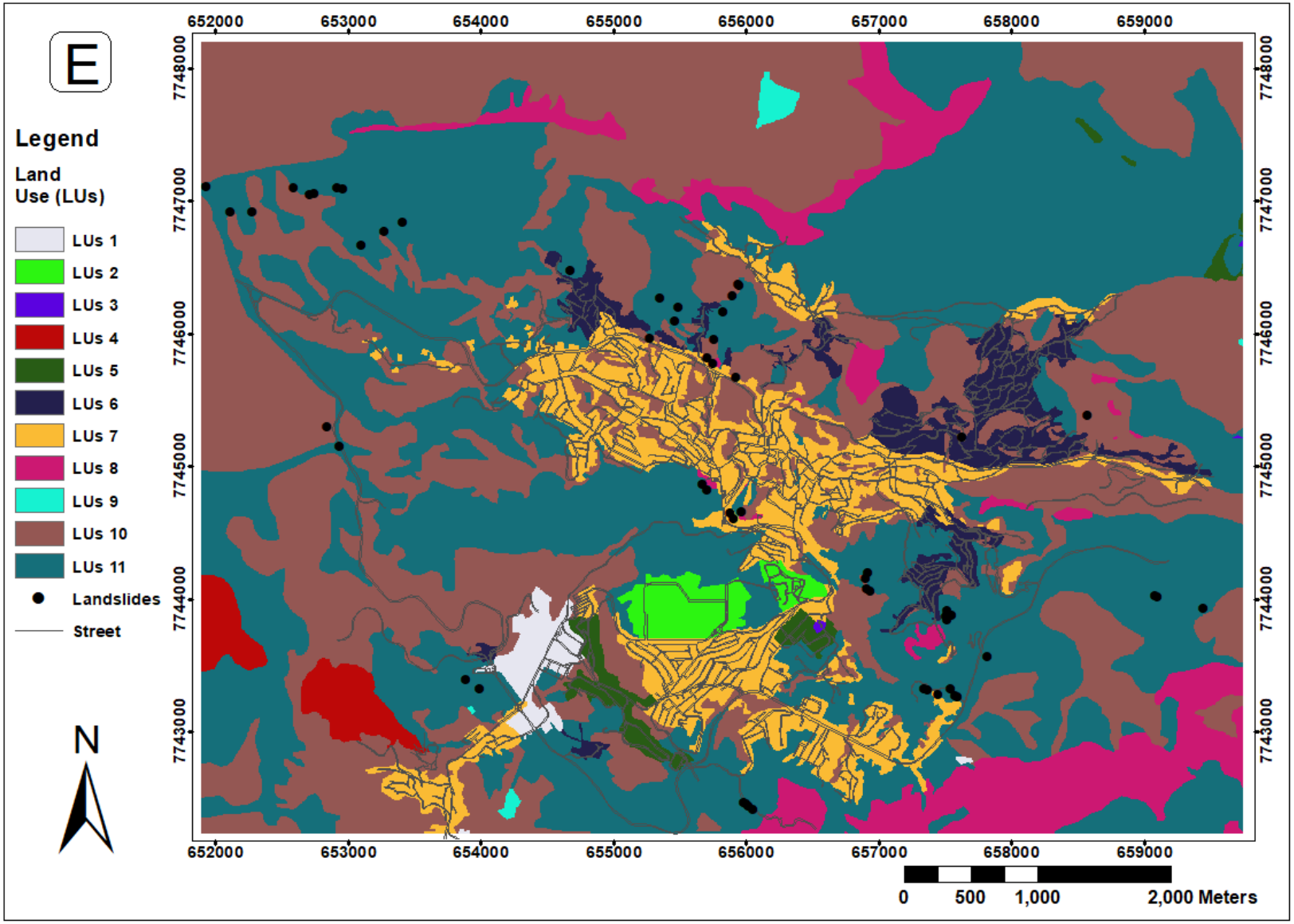
E
Legend
Land
Use (LUs)
LUs 1
LUs 2
LUs 3
LUs 4
LUs 5
LUs 6
LUs 7
LUs 8
LUs 9
LUs 10
LUs 11
Landslides
Street
N
652000
653000
654000
655000
656000
657000
658000
659000
7748000
7747000
7746000
7745000
7744000
7743000
0
500
1,000
2,000 Meters

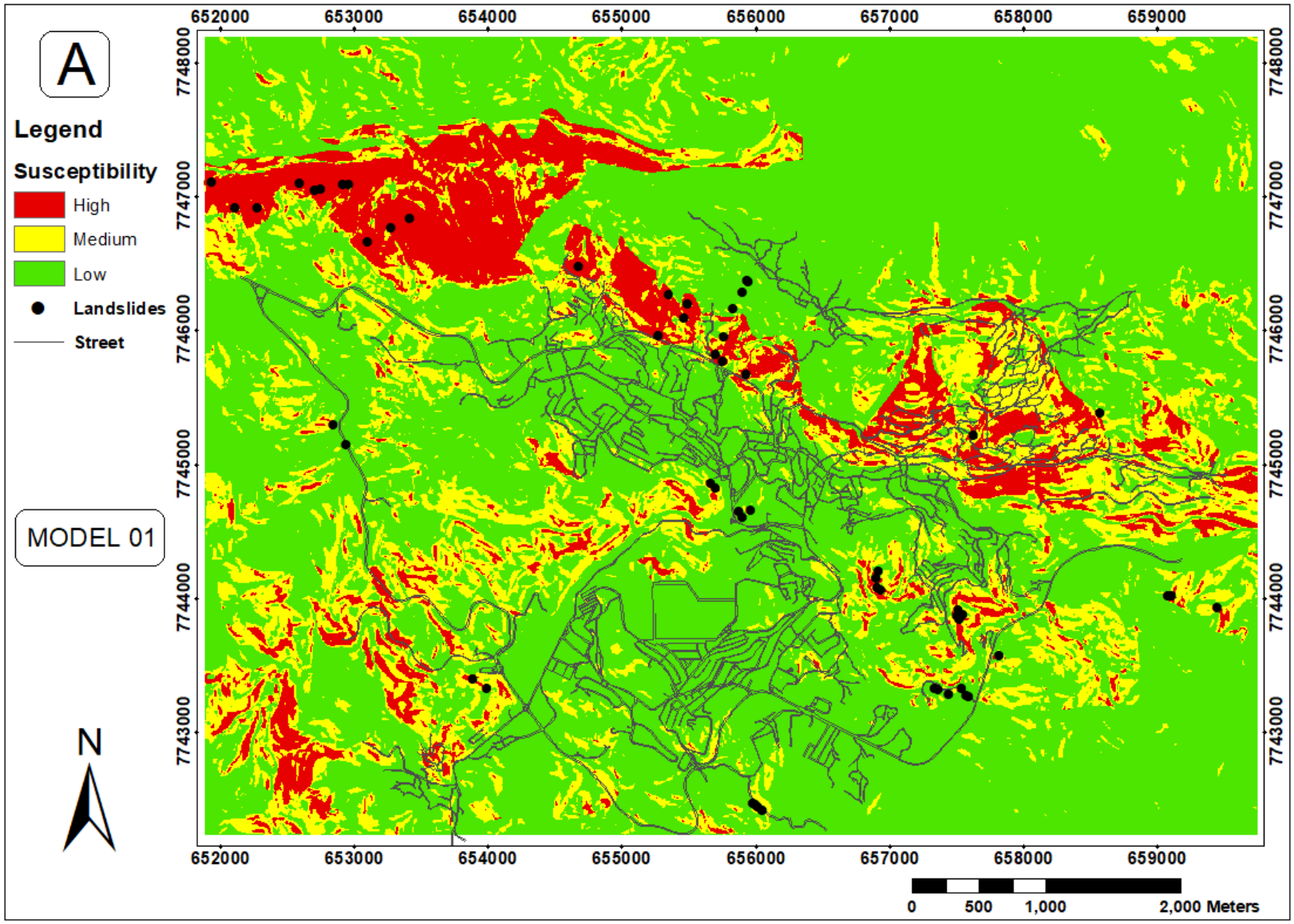
A
Legend
Susceptibility
High
Medium
Low
Landslides
Street
MODEL 01
N
652000
653000
654000
655000
656000
657000
658000
659000
7748000
7747000
7746000
7745000
7744000
7743000
0
500
1,000
2,000 Meters

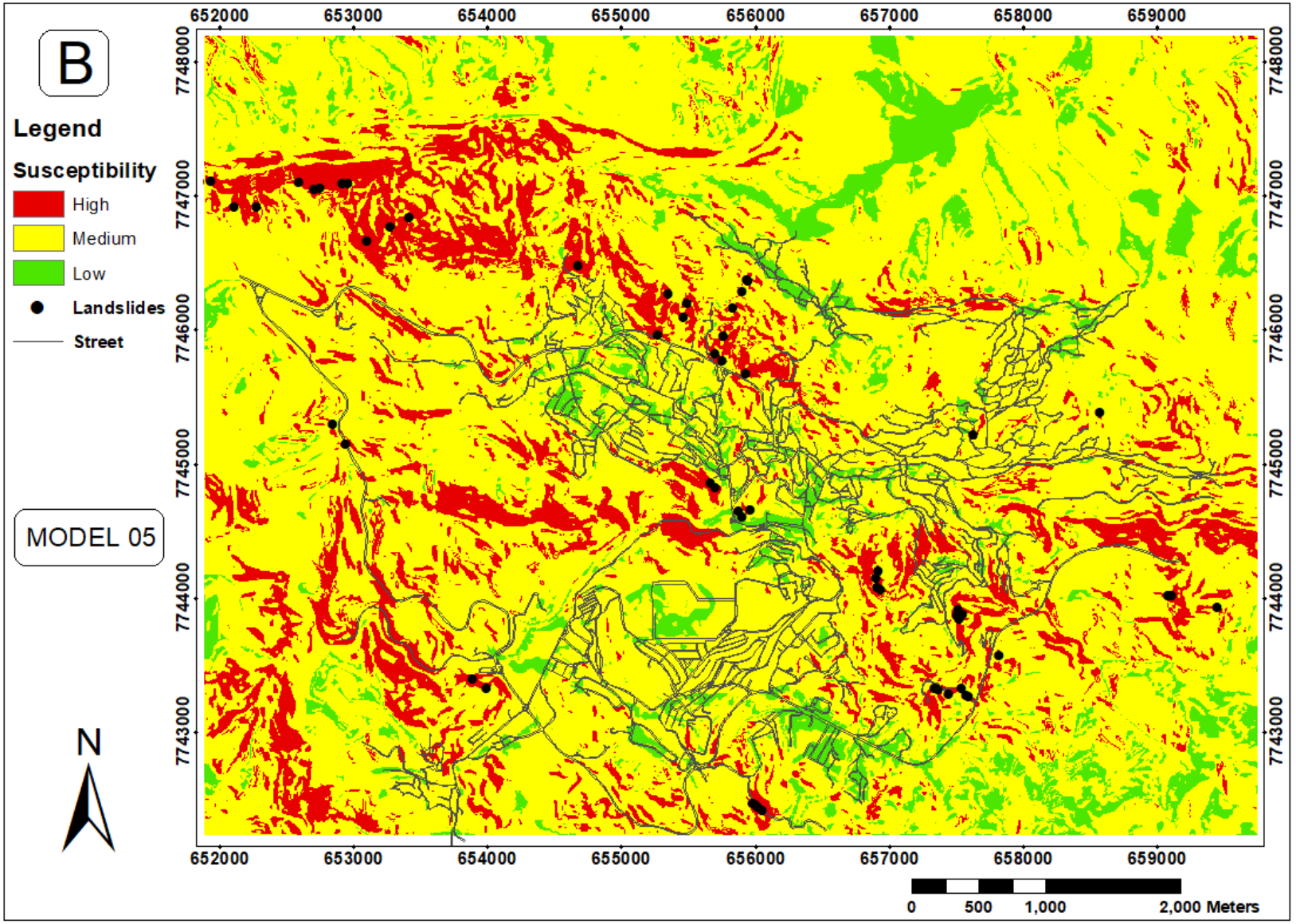
B
Legend
Susceptibility
High
Medium
Low
Landslides
Street
MODEL 05
N
652000
653000
654000
655000
656000
657000
658000
659000
7748000
7747000
7746000
7745000
7744000
7743000
0
500
1,000
2,000 Meters

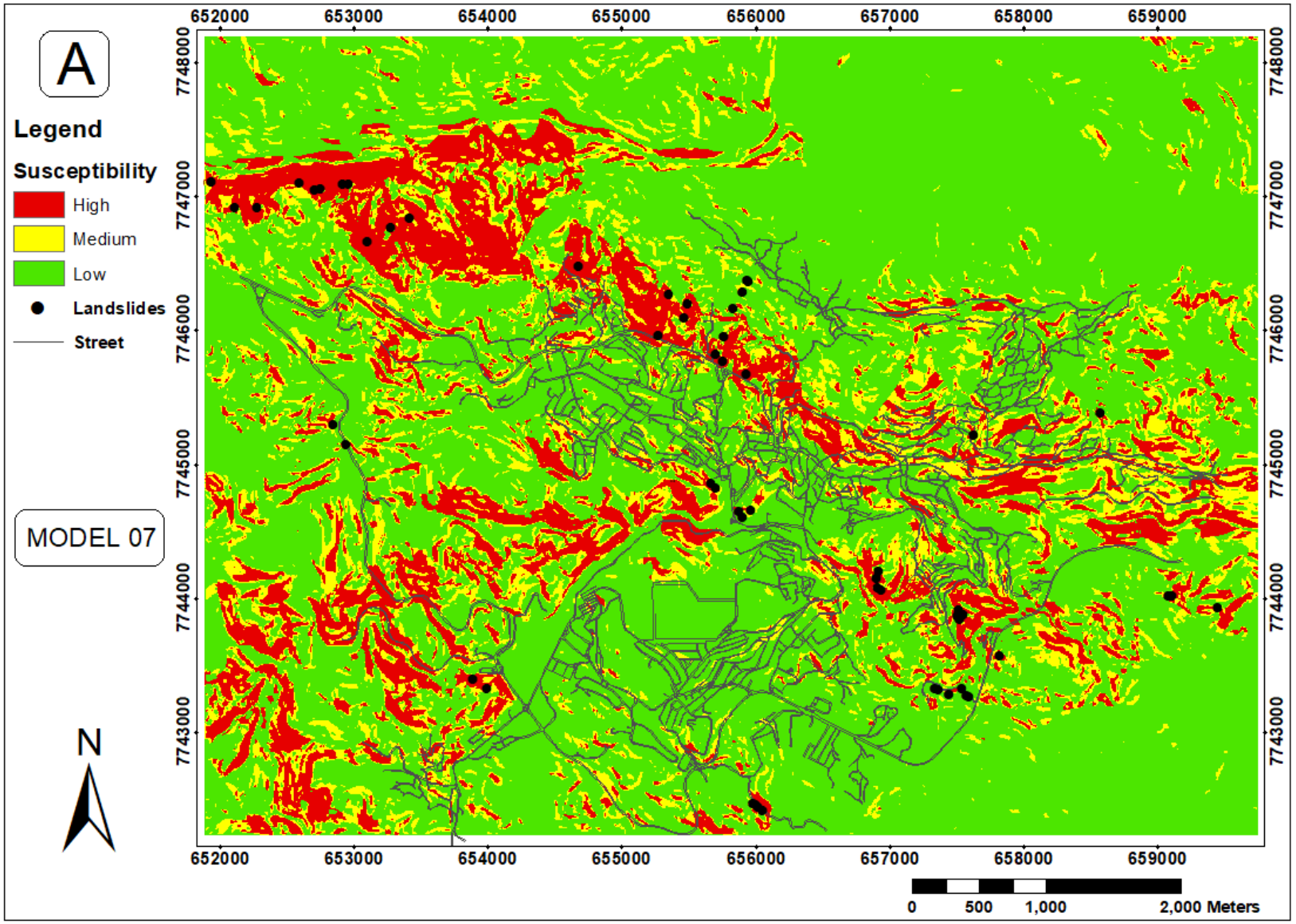
A
Legend
Susceptibility
High
Medium
Low
Landslides
Street
MODEL 07
N
652000
653000
654000
655000
656000
657000
658000
659000
7748000
7747000
7746000
7745000
7744000
7743000
0
500
1,000
2,000 Meters

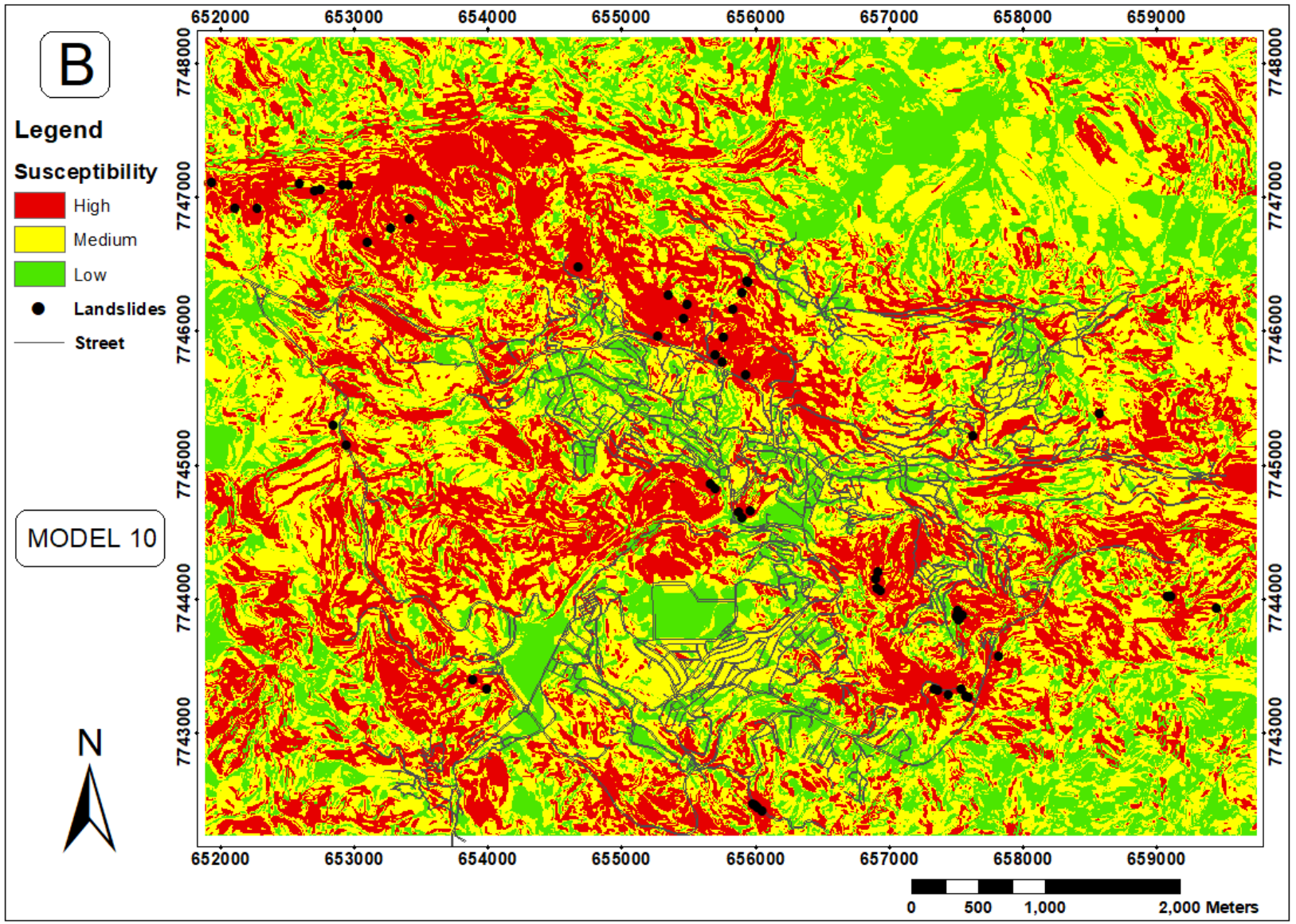
B
Legend
Susceptibility
High
Medium
Low
Landslides
Street
MODEL 10
N
652000
653000
654000
655000
656000
657000
658000
659000
7748000
7747000
7746000
7745000
7744000
7743000
0
500
1,000
2,000 Meters

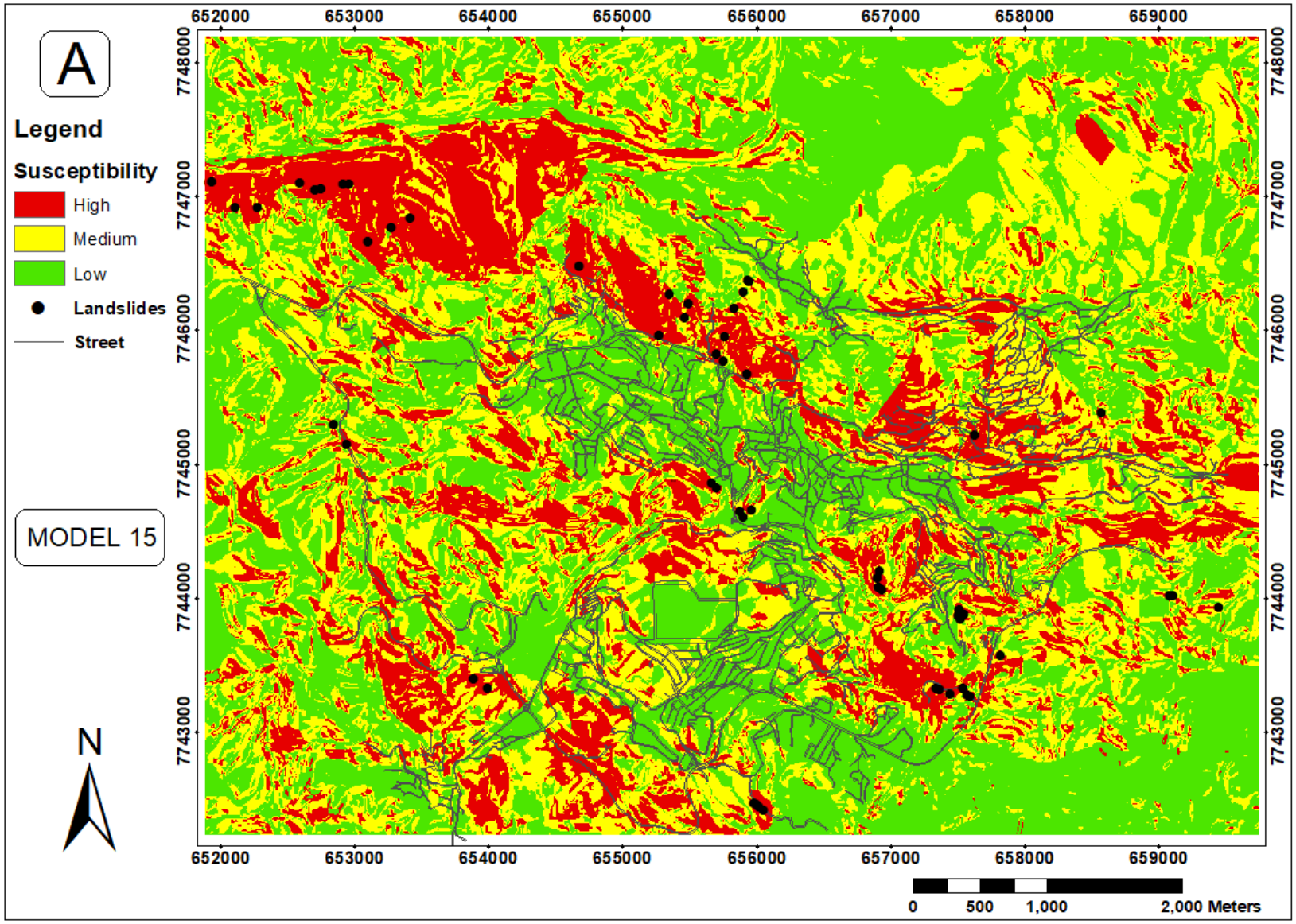
A
Legend
Susceptibility
High
Medium
Low
Landslides
Street
MODEL 15
N
652000
653000
654000
655000
656000
657000
658000
659000
7748000
7747000
7746000
7745000
7744000
7743000
0
500
1,000
2,000 Meters

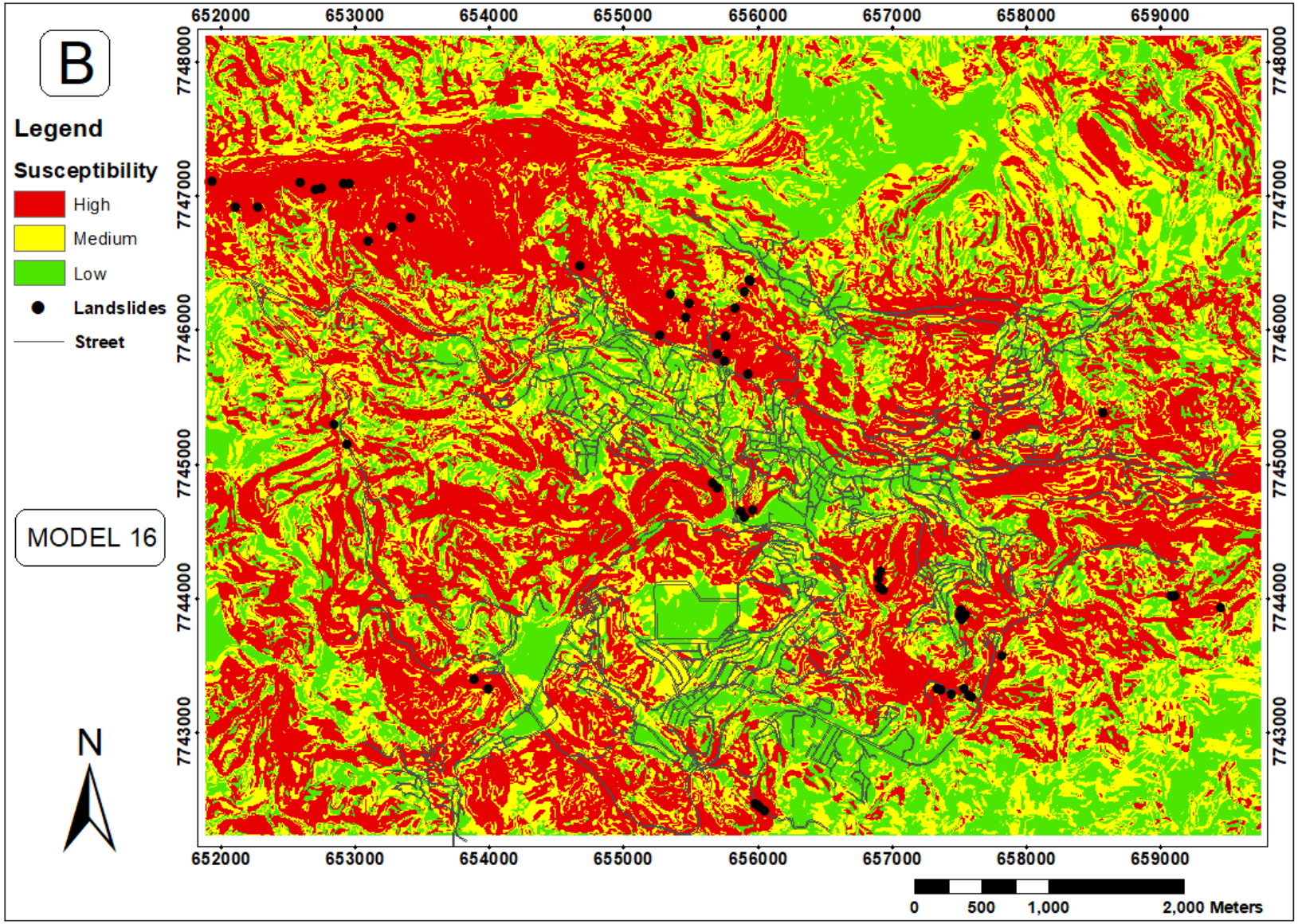
B
Legend
Susceptibility
High
Medium
Low
Landslides
Street
MODEL 16
N
652000
653000
654000
655000
656000
657000
658000
659000
7748000
7747000
7746000
7745000
7744000
7743000
0
500
1,000
2,000 Meters